Q. J. R. Meteorol. Soc. (1998), **124**, pp. 705–732

A first-order closure for disturbed plant-canopy flows, and its application to winds in a canopy on a ridge

By JOHN D. WILSON[1]*, JOHN J. FINNIGAN[2] and MICHAEL R. RAUPACH[2]
[1]*University of Alberta, Canada*
[2]*CSIRO Land and Water, Australia*

(Received 2 May 1996; revised 20 December 1996)

SUMMARY

To calculate disturbed wind flows in plant canopies, we studied a variant of the $K \propto \lambda k^{1/2}$ first-order closure (where K is the eddy viscosity, k is the turbulent kinetic energy calculated from its simplified governing differential equation, and λ is an algebraic length-scale). We compare numerical solutions using this closure (which admits only three empirical constants) with earlier observations of mean wind, shear stress, and turbulent kinetic energy in three, quite different, uniform canopy flows, and in disturbed canopy flow over a ridge. The closure performs as well as or better than the solutions of others based on modifications of the 'k-ϵ' closure, where ϵ is the rate of dissipation of k.

KEYWORDS: Boundary layer Orography Turbulence Vegetation

1. INTRODUCTION

Arguably the most important scientific challenge facing micrometeorology, is to improve our understanding of, and means to calculate, the spatial variation of the turbulent wind flow over complex terrain. This is necessary not only to improve surface parametrizations within larger-scale models, but also to make advances in related applied sciences, such as air pollution, hydrology, and forestry. From the perspective of numerical fluid mechanics and the governing conservation equations, the fundamental problem is that of 'turbulence closure'. This work arose from our exploration of the following question, prompted by the wind-tunnel experiment of Finnigan and Brunet (1995)—what is the simplest turbulence closure that will adequately describe changes to the mean wind field, particularly very close to the ground, in flow over hilly, forested terrain? The possibility of interpreting the spatial pattern of tree 'windthrow' (e.g. Wilson and Flesch 1996, who studied turbulence and remnant tree motion in forest clearings of varying widths) illustrates the value of being able to model such flows.

Finnigan and Brunet studied changes to the mean wind and turbulence in flow through a model plant canopy on a wind-tunnel ridge ('Furry Hill'). Striking *qualitative* differences were observed between the shapes of the mean wind profiles, $U(z)$, at different points on the ridge. In the case of a canopy on level ground, $U(z)$ is characterized by strong shear near the canopy height ($z = h_c$), and an associated inflexion point in the wind profile. But on the upwind slope of Furry Hill that inflexion point was weak or even absent, while at the hilltop it was markedly accentuated. Eddies originating from the inflexion-point wind profile are an important component of canopy turbulence (Raupach *et al.* 1996), and so these disturbances of the *form* of the wind profile in flow over a forested hill may be very important. In any case, the Furry Hill observations determined a pattern of mean wind variation that a useful closure must capture.

Our first step was to extend the Jackson–Hunt (1975) linear analytic theory to cover this case, by adding a canopy layer beneath the inner layer. But upon testing that calculation against the Furry Hill observations we found the assumption of small disturbances was invalid. We therefore embarked on nonlinear numerical solutions, and the bulk of this report

* Corresponding author: University of Alberta, Department of Earth and Atmosphere Sciences, Edmonton, Alberta, Canada T6G 2E3.

describes a variation, applicable specifically to canopy flow, of the familiar $K \propto \lambda k^{1/2}$ first order closure (where K is the eddy viscosity, k is the turbulent kinetic energy (TKE) calculated from a simplified governing differential equation, and λ is an algebraic length-scale). Using this closure, we will demonstrate good agreement of numerical solutions with observations of three, quite different, uniform canopy flows, and encouraging agreement with the Furry Hill observations of flow over a ridge.

But it will occur to many readers that our use of a first-order closure for disturbed canopy flow begs strong justification! We will review the context of our choice, acknowledging at the outset our preference for simplicity in a scientific model. There is some consensus that first-order closure suffices to explain changes to the *mean* flow well above the canopy (indeed, this is implied by the success of the Jackson–Hunt theory). According to Ayotte *et al.* (1994, page 30), 'mean-flow over hills generally shows only a weak sensitivity to the concomitant turbulence field'; and from Ying *et al.* (1994) we have that 'It has been shown in many studies that in steady-state, neutrally-stratified ABL* flow over topography, the mean velocity changes are relatively insensitive to the turbulence closure scheme'. However K-theory is considered unable to explain the observed changes to the *turbulence* over a hill, even above any canopy: thus (Taylor *et al.* 1987, page 112) 'subtleties of the turbulence model are of importance to the turbulence structure but appear to have little influence on the mean flow'.

Will these findings hold true *within* a canopy on a hill? Several factors render canopy flows among the most complex so far studied: extreme vertical inhomogeneity of the velocity statistics; the strongly non-Gaussian nature of those statistics; domination of the transport process by occasional energetic 'sweeps' of air from above; and distributed source/sink distributions for momentum, heat, water vapour (etc.) that imply source terms in the governing equations for statistics of any order. The impact of this complexity of canopy flow on the applicability of K-theory is severe—in a plant canopy mean fluxes are observed *sometimes* to be directed against the corresponding mean gradient (e.g. Denmead and Bradley 1985). This is understood (Raupach 1987; Wilson 1989) to be due to the action of the energetic 'large' eddies, with length-scales of the order of the canopy height, on a vertically extensive source distribution. Raupach (1987) adopted a Lagrangian viewpoint to show that the effective eddy diffusivity at a point in the canopy flow had a 'diffusive' contribution, representing the flux from sources at distances exceeding the local Lagrangian integral length-scale, and a 'non-diffusive' contribution from nearby sources. The non-diffusive part of the eddy diffusivity was generally quite a small perturbation on the diffusive part, but was sufficient to produce the observed counter-gradient transport, given a conducive source distribution. Of course, counter-gradient transport cannot be entertained within K-theory.

In the Eulerian framework, non-local, non-diffusive behaviour can be reproduced by higher-order closures (there remains in principle the difficulty that such models invoke gradient diffusion at a higher order). To this end Wilson and Shaw (1977) and Wilson (1988) calculated canopy winds using second-order closure, while Meyers and Paw U (1986) introduced a third-order closure. Even for a uniform canopy, this results in considerable complexity; although, if for no other reason than the introduction of many closure coefficients, it is possible to match quite arcane details of measured flows.

In the present work it seemed reasonable as a first step to explore K-theory, ignoring the non-diffusive, non-local part of the diffusivities and relaxing our expectation that the resulting description should work well at *every* point of the flow, in favour of reproducing the overall character of the flow with minimal complexity. We were inclined to over-

* Atmospheric boundary layer.

look details such as the TKE partitioning (σ_u^2:σ_v^2:σ_w^2) and to avoid complicated turbulence schemes, however popular, whose basis is especially weak in the case of a canopy flow (e.g. the ϵ-equation, where ϵ is the rate of dissipation of TKE).

Now in what is to our knowledge the only previous computation of disturbed canopy winds on a hill, Kobayashi *et al.* (1994) compared wind-tunnel simulations with calculations using the first-order 'k-ϵ' closure. The 'standard' ϵ-equation (Launder and Spalding 1972) provides a 'successful' length-scale $k^{3/2}/\epsilon$ in many simple flows, but, in view of what is known about TKE transformation/dissipation pathways in a canopy (Shaw and Seginer 1985; Wilson 1988; Kaimal and Finnigan 1994, page 97), it is hardly surprising that the standard ϵ-equation resulted in a poor calculation of the measured TKE and shear stress.

Svensson and Haggkvist (1990), Green (1992), Kobayashi *et al.* (1994) and Liu *et al.* (1996) have described similar modifications of the k-ϵ model, to account for plant drag. However such k-ϵ closures give predictions that are sensitive to details of ambiguous choices (e.g. Liu *et al.* Fig. 9) and are, at best, of a quality comparable to those of the present, simpler scheme. Thus rather than modify the ϵ-equation, we preferred to impose a length-scale that reflects the known characteristics of canopy eddies. Although we agree with Ying *et al.* (1994, page 402) that 'there is little evidence to support the belief that the length-scale specifications used in one-equation models (where only the transport equation for turbulent kinetic energy is solved) are sufficiently universal for (separated, recirculating) flows', we contend (and indeed prove) that in the present context a rationally formulated length-scale will equal or outperform an inappropriate ϵ-equation. Please note though, that we have not sought here to treat any leeward separation region.

This ends our 'justification' for using K-theory, and our particular version of it. We now outline a $K \propto \lambda k^{1/2}$ closure which, as we use it, admits three unknown coefficients. These we have determined by optimising agreement of calculated mean wind (U), shear stress (τ), and TKE (k) profiles with those observed in the equilibrium canopy flow upwind of Furry Hill. Without alteration those values also resulted, as we will show, in quite good simulations of other very different uniform canopy flows, and of the disturbed wind and turbulence in and above a canopy on a hillside.

2. Governing equations

We used simplified governing equations for a neutrally stratified boundary-layer flow, in which velocity statistics are invariant along the crosswind (y) direction (2-dimensional mean flow). Our focus is wind in a plant canopy, and so our interest is in the surface layer. However, much of the available data are from the wind-tunnel, wherein the constant-stress layer above the canopy is shallow, or even non-existent. Thus we allowed a background along-wind pressure gradient, to balance any vertical gradient in above-canopy shear stress $\partial_z\langle u'w'\rangle$ (u' and w' are departures from the mean horizontal wind U and mean vertical velocity W; and $\langle\ \rangle$ denotes an average), and also to account for vertical variation in TKE above a uniform wind-tunnel canopy. TKE (k) in our treatment represents the kinetic energy of eddies in a spectral range that *excludes* the small, wake-scales (that are rapidly dissipated). Thus, in the canopy, drag on plants operates as a net *sink* for TKE.

Governing equations applicable to both uniform and disturbed terrain can be derived by a transformation of the usual momentum equations (under the Boussinesq approximation) into non-orthogonal, terrain-following coordinates (x, z), where z is height above the *local* terrain surface, the absolute height of which is written $h(x)$. U and W are retained as the dependent variables (i.e. velocities are referred to fixed Cartesian axes), but it is

convenient to define:

$$W^* = W - h_x U, \tag{1}$$

where h_x is the derivative of h with respect to x. W^* is the *difference* between local vertical velocity and the projection of the horizontal velocity onto the local normal to the hill. For reasons which will become clear later, we did not transform the z-axis in the way that is often done to achieve an upper coordinate surface which is horizontal. In terms of W^*, the continuity equation may be written:

$$\frac{\partial U}{\partial x} + \frac{\partial W^*}{\partial z} = 0. \tag{2}$$

The momentum equations, written in transport form (which is advantageous for ensuring proper conservation in the numerical integrations to follow), are:

$$\frac{\partial}{\partial x}(U^2 + \sigma_u^2 + P) + \frac{\partial}{\partial z}(W^* U + \langle u'w' \rangle) = \frac{\partial}{\partial z}(h_x(\sigma_u^2 + P)) + S_u, \tag{3}$$

and

$$\frac{\partial}{\partial x}(UW^* + \langle u'w' \rangle) + \frac{\partial}{\partial z}(W^{*2} + \sigma_w^2 + P) = h_x \frac{\partial \langle u'w' \rangle}{\partial z} - \frac{\partial}{\partial x}(h_x U^2) - \frac{\partial}{\partial z}(h_x W^* U). \tag{4}$$

Here P is the mean kinematic pressure, σ_u^2 is the variance of the total horizontal velocity $U + u'$ about the mean (U); σ_w^2 is the variance of the total vertical velocity $W + w'$ about the mean (W); and $\langle u'w' \rangle$ is the turbulent kinematic shear stress (τ). The source term $S_u(x, z) = -c_d(z)a(x, z)U|U|$ parametrizes drag on vegetation; $c_d(z)$ is a bulk drag coefficient, and $a(x, z)$ is the plant area density. The left-hand sides of these equations preserve the form familiar in Cartesian coordinates, but there are extra terms on the right-hand sides (r.h.s.) arising from the transformation, which we shall shortly drop.

We also used a transformed (and simplified) TKE equation:

$$\frac{\partial}{\partial x}(Uk) + \frac{\partial}{\partial z}(W^* k) = -\langle u'w' \rangle \frac{\partial U}{\partial z} + PT_i - \epsilon. \tag{5}$$

PT_i represents the sum of the pressure and turbulent transport terms; ϵ is the rate of dissipation of TKE; and we have simplified shear production.

In the wind flow simulations to be reported, the pressure gradient was either trivial (uniform canopy flows) or, in the case of the Furry Hill experiment, provided. Thus we will make no further use of the W-momentum equation; vertical velocity can be eliminated using the continuity equation.

(*a*) *Inadequacy of linear treatment*

Jackson and Hunt (1975; hereafter JH) provided an analytical theory of the disturbance in mean wind speed that occurs when a neutrally stratified boundary-layer flow encounters a low, smooth ridge. Despite its restriction to small disturbances, this work has played an important role in interpretation of observations, and has permitted a deeper understanding of 'hillflow' than available from numerical solutions; e.g. JH contributed the simplifying concept that the hillflow is comprised, in essence, of two layers: a highly-sheared, near-ground stream; and above that an irrotational, inviscid outer stream, whose blockage by the hill sets up the pressure field *driving* the inner layer.

As potentially the simplest description of wind changes in a canopy on a hill, we explored a number of ways to add a canopy layer below the base of the JH inner layer. Briefly, this involved a displacement of the height coordinate ($z \to z - d$), and the introduction of matching conditions at canopy height $z = h_c$ between the canopy layer and the JH inner layer. Requirements of continuity of the wind speed and shear stress across h_c in effect replaced the lower-boundary conditions of the JH treatment. We linearised the momentum budget of the canopy layer, by introducing an exponential background wind profile $U_0(z)$, and we assumed a height-independent mixing-length, λ_0, within the canopy (λ_0 turned out necessarily to also be independent of x, for proper matching to the JH inner layer). These solutions did not agree very well with the observed winds in the canopy on Furry Hill. The basic difficulty can be revealed by considering the force balance deep in the canopy.

Vertical coupling in thin shear flow is primarily due to the turbulent vertical momentum flux, τ, which as is well known does not penetrate deeply into a dense canopy. Thus the flow in the base of a deep, dense canopy is vertically-decoupled from the flow aloft (of course the flow deep in the canopy is 'advectively' coupled, i.e. in regions where $\partial\tau/\partial z$ is small, the deep-canopy flow reflects advection from regions where the coupling was strong). Under such conditions the mean momentum budget deep in the canopy is:

$$U\frac{\partial U}{\partial x} = -\frac{\partial P}{\partial x} - c_d a U|U|, \tag{6}$$

and the wind speed $U(x)$ is accordingly determined by the pressure field. In the absence of advection, this reduces to the balance between pressure gradient and drag proposed by Holland (1989) for the base of a deep, dense canopy.

Does Eq. (6) explain the observed wind variations deep in the canopy on Furry Hill? The wind-tunnel ridge had topographic contour:

$$h(x) = \frac{H}{1 + \left(\frac{x}{L}\right)^2}, \tag{7}$$

where H is the hill height and L the hill half-length (a 'Witch of Agnesi' ridge). For that case the JH solution for the pressure field in the inner layer is:

$$\frac{P_{JH}}{\rho u_{*0}^2} = \frac{1}{k_v^2}\frac{H}{L}\ln^2\left(\frac{L}{z_0}\right)\frac{\left(\frac{x}{L}\right)^2 - 1}{\left(1 + \left(\frac{x}{L}\right)^2\right)^2}, \tag{8}$$

where k_v is von Kármán's constant and u_{*0} is the upstream (equilibrium) friction velocity. Figure 1(a) compares the observed pressure over Furry Hill ($L = 0.42$ m, $H = 0.15$ m) against the JH pressure field for a hill of effective height $H' = 0.08$ m (the JH solution for the actual ridge predicts a more extreme pressure variation than was observed). While P_{JH} underestimates the adversity of the observed pressure gradient at $x/L < -1.5$, it matches well the overall pressure fall at hilltop. The very strongly adverse $\partial_x P_{JH}$ leeward of hilltop would cause prompt reversal. It is not seen in the Furry-model flow for precisely that reason—the model flow featured a large separated region behind the crest.

Figure 1(b) compares the variation (on the upwind face of the hill) of the observed winds in the canopy at $z/h_c = (0.17, 0.5)$ against numerical solutions $U(x)$ to Eq. (6), or

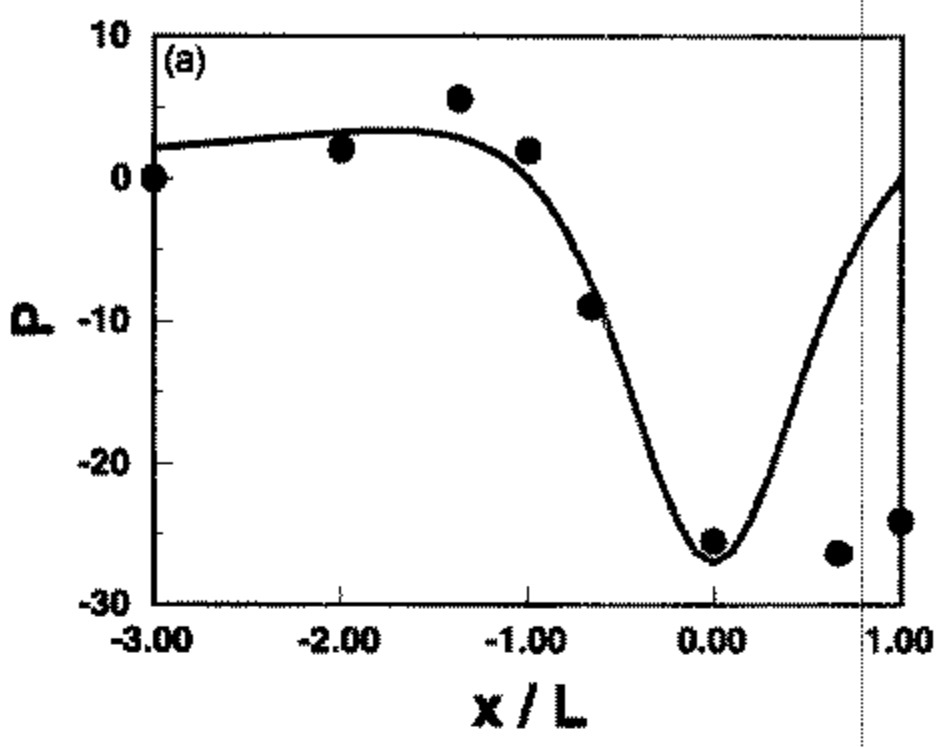

Figure 1. (a) Comparison of observed mean pressure (•, normalized on ρu_{*0}^2) over Furry Hill ($L = 0.42$ m, $H = 0.15$ m), with the JH theoretical pressure field $P_{JH}(x)$ for the inner layer on a ridge with scales $L = 0.42$ m, $H = 0.08$ m, $z_0 = 0.0036$ m. (b) Mean wind speeds U/u_{*0} observed in the canopy on Furry Hill, versus solutions $U(x)$ of a nonlinear, one-dimensional U-momentum budget that includes only canopy drag, forcing pressure gradient, and advection. Also shown (light solid lines) are a family of solutions of the *linearized* one-dimensional budget. All solutions are 'driven by' the pressure field P_{JH} of Fig. 1(a), and use $c_d aL = 2.86$, the observed value. The nonlinear solutions are pinned to the observed far-upstream deep-canopy wind ($U_0/u_{*0} = 1, 1.5$). The family of linearized solutions used $U_0/u_{*0} = (0.5, 0.75, 1.0, 1.25, 1.5)$. See text for further explanation.

rather a slight modification of it:

$$U\frac{\partial U}{\partial x} = -\frac{\partial P_{JH}}{\partial x} - c_d a(U|U| - U_0^2) + K^*\frac{\partial^2 U}{\partial x^2}. \tag{9}$$

$c_d a U_0^2$ is a background stress gradient; in its absence, this model cannot reproduce the observed far-upwind deep-canopy wind. The artificial diffusion term ($K^*/u_{*0}L$, set equal to 0.001) merely suppresses computational instability. From the reasonable agreement of the nonlinear solution with the observed wind, it is evident that the flow deep in the canopy is indeed virtually decoupled from the flow aloft, as others have suggested. In fact, where the pressure gradient is large on Furry Hill one may neglect advection, and obtain a good estimate of the deep-canopy mean wind speed algebraically from the known pressure field—as suggested by Holland (1989). Froml the form of Eq. (6), Finnigan and Brunet (1995) reasoned that within the canopy, due to the drag on plant parts, there is constant readjustment of the wind towards equilibrium with the pressure field, with distance constant $(c_d a)^{-1}$. In contrast, above the vegetation the lack of damping permits freer response to ∇P and, according to Finnigan and Brunet, this is the cause of the changing magnitude of the wind shear at canopy top.

Returning to our main point, also shown on Fig. 1(b) are a family of solutions for $U(x)$ that result upon *linearization*,

$$U(x) = U_0 + U'(x), \tag{10}$$

where U' is the mean wind perturbation induced by the hill, and U_0 is the approach speed. The linearized solutions overestimate changes in the wind near the ground. Thus the wind changes in the plant canopy on Furry Hill demand a nonlinear treatment.

(*b*) *Closure*

As we emphasized earlier, our intent was to uncover a simple but workable closure for disturbed canopy flows. Thus we use K-theory, which we write down in the form given

by Monin and Yaglom (1977; section 6.3) for arbitrary 3-dimensional flows:

$$\langle u_i' u_j' \rangle = \frac{2}{3} k \delta_{ij} - K \left(\frac{\partial U_i}{\partial x_j} + \frac{\partial U_j}{\partial x_i} \right), \tag{11}$$

where δ_{ij} is the Kroneker delta. This scalar-viscosity closure, whose merit is correct symmetry, is often modified (introducing empirical parameters such as c_u below) to permit distinction between the normal stresses in an undisturbed flow, viz.

$$\langle u'^2 \rangle = c_u k - 2K \frac{\partial U}{\partial x}. \tag{12}$$

The concept that $\langle u'^2 \rangle$ is controlled by U-inhomogeneity has little to recommend it. In any case, experimental evidence suggests that in most disturbed thin shear-layer flows (i.e. flows wherein shear strains $\gg$ normal strains) normal stress gradients play a much smaller role than shear stress gradients. Their inclusion via the above closure does have the purely computational advantage of providing diffusion terms. For simplicity, and in view of the weak basis for Eq. (12), we neglected the normal stress gradients; also, because vertical shear is dominant in thin shear flow, we simplified the shear stress closure to:

$$\langle u' w' \rangle = -K \frac{\partial U}{\partial z}. \tag{13}$$

To ensure numerical stability, we added diffusion terms where diffusion was otherwise absent. We regard these as artificial, and signify the artificial diffusivity as K_a, which is very small.

(c) *Parametrization of eddy viscosity*

For reasons indicated in the Introduction, we chose to specify the eddy viscosity as:

$$K = \lambda(x, z) \sqrt{c_e k(x, z)}, \tag{14}$$

where k was obtained from the simplified transport Eq. (5), and the length-scale $\lambda(x, z)$ was specified algebraically. The constant c_e is the equilibrium shear-stress/TKE ratio (u_{*0}^2/k_0) immediately above the canopy, which if evaluated in the local equilibrium region varies only slightly from one wall-shear layer to another. We defined an eddy diffusivity $K_k = \mu K$ to parameterize the transport term PT_t in the TKE Eq. (5).

According to Launder and Spalding (1972), this 'one-equation model of turbulence', which has been used widely (e.g. to calculate flow over hills, Taylor 1977), originated with L. Prandtl in 1945 and, 'in most circumstances, one-equation models are only marginally superior to Prandtl's mixing-length model'. However, that assessment derives from studies of turbulence typical of engineering flows: wall-shear layers; decaying homogeneous turbulence; jets and wakes. In our more complex case of a canopy flow, involving form drag and terms of similar origin in governing equations for all statistics, we preferred to keep an open mind on the issue, and to proceed from a simple starting point. The more complex first- or second-order closures preferred by Launder and Spalding introduce numerous closure coefficients, and in their application to canopy flows it is difficult to differentiate profoundness of the set of closure assumptions from mere flexibility due to those coefficients. Of course, we recognise the principle that the constants of a closure, once established by optimization with respect to simple test flows, should be left unchanged in

their application to more complex flows. However, as we indicated earlier, popular engineering closures, such as the k-ϵ model (Launder and Spalding 1972) or the second-order closure of Launder *et al.* (1975), both of which include an ϵ-equation to relieve the need for specification of a length-scale, will not carry over to canopy flows without modification. This is because of the extra processes involving vegetation drag (witness the rather poor performance of the model of Kobayashi *et al.* 1994). And while the mechanisms of production, destruction and inter-scale transformation of TKE in a canopy are partially understood (Shaw and Seginer 1985; Kaimal and Finnigan 1994, page 97), we do not yet have a meaningful ϵ-equation for canopy flows. Thus our preference is for an algebraic parametrization of the length-scale and of the sink (ϵ) for resolved-scale TKE, to avoid proliferation of closure constants, and 'black-box' equations.

In specifying the length-scale, we wished to reproduce the observed characteristic (Kaimal and Finnigan 1994, Fig. 3.13) of a constant length-scale across much of the upper canopy ($\lambda < k_v h_c$, where $k_v = 0.4$ is von Kármán's constant), and some distance above but near the canopy an 'inertial sublayer' wherein $\lambda \propto (z - d)$, d being the displacement height. As a result of our analytic treatments of the canopy on a hill, we wished also to allow the length-scale to (realistically) vanish on the ground, i.e. as $z/h_c \to 0$. Thus we wrote $\lambda = \max(\lambda_i, \lambda_o)$, where:

$$\frac{1}{\lambda_i} \equiv \frac{1}{k_v z} + \frac{1}{\lambda_c} \quad \text{and} \quad \frac{1}{\lambda_o} \equiv \frac{1}{k_v (z - d)} + \frac{1}{L_\infty}. \tag{15}$$

The 'outer' scale λ_o recognizes the displacement (of equilibrium structure) due to the canopy and, through the imposed limiting (i.e. maximum permitted) value L_∞, the fact of a restricted depth to the inertial sublayer in a wind-tunnel boundary layer. In the case of a deep constant-stress layer, e.g. in our simulations of the Elora field data (Wilson 1988), we set $L_\infty = \infty$. The 'inner' scale λ_i recognizes both the limitation imposed on eddy size by proximity to the ground, and the presence of the canopy. Raupach *et al.* (1996) have suggested that the strength of the wind shear at 'canopy height'* is critical to eddy transport within a canopy, defining a 'shear length-scale':

$$L_s = \frac{U(h_c)}{(\partial U/\partial z)_{h_c}}. \tag{16}$$

Accordingly we specified the upper limit to the 'canopy' length-scale either as:

$$\lambda_c = c L_s, \tag{17}$$

or as:

$$\lambda_c = c L_s^* = c\sqrt{k(h_c)} \left(\frac{\partial U}{\partial z}\right)_{h_c}^{-1}, \tag{18}$$

where L_s^* is an alternative length-scale; in either case, c is an unknown constant of proportionality, or 'closure constant', which we will subsequently determine. Equation (18) has an advantage in principle over Eq. (17), in that in the limit of a very sparse canopy, it specifies $\lambda_c(h_c) \propto k_v(h_c - d)$, whereas Eq. (17) has a less elegant low canopy-density

* Raupach *et al.* suggested h_c might be unambiguously *defined* as being the height (h_{ip}) of the inflection-point of the mean wind profile. Within our treatment and closure there is no compulsion to define canopy height as that height (h_{mx}) above which plant area density vanishes, although we have done so for all simulations reported here. The suggestion that one defines $h_c = h_{ip}$ can, and probably should, be accommodated in cases where h_{ip} is distinctly lower than h_{mx} (e.g. the Rivox spruce canopy, wherein h_{ip} occurred at approximately the *median* tree height; Gardiner 1994).

limit. In all simulations to be shown here we have used Eq. (18). However there is no decisive advantage to using $k^{1/2}(h_c)$ instead of $U(h_c)$ as the velocity-scale for defining L_s. Our findings can be reproduced using Eq. (17), though with $c \approx 0.5$ rather than $c = 1.0$, the latter value resulting from the calibration to follow.

The TKE dissipation rate was written as $\epsilon = \max(\epsilon_{cc}, \epsilon_{fd})$ where:

$$\epsilon_{cc} = \frac{(c_e k)^{3/2}}{\lambda}, \quad \epsilon_{fd} = \alpha c_d a U k. \tag{19}$$

The term ϵ_{cc} is the standard parametrization for viscous dissipation, the only TKE sink above the canopy (ϵ_{cc} balances shear production of TKE, in the local equilibrium layer well above the canopy). Our specification for ϵ_{fd} ('form drag'), which converts resolved TKE to the small, rapidly dissipated 'wake-scales', can be justified on physical grounds (e.g. Wilson 1988). We expect α is O(1), but its exact value depends on the partitioning of k among the components (u', v', w'), and on the spectral division of TKE into our resolved band (k) and the irrelevant band of finer wake-scales.

We will henceforth use the equations in non-dimensional form, using for scales h_c, and the friction velocity u_{*0} derived from the equilibrium shear stress at $z = h_c$. The governing equations for U and k in terrain-following coordinates, incorporating the simplifications above, and omitting the superscript on our 'vertical' velocity, are:

$$\frac{\partial}{\partial x}\left(U^2 - K_a \frac{\partial U}{\partial x}\right) + \frac{\partial}{\partial z}\left(UW - K\frac{\partial U}{\partial z}\right) = -\frac{\partial P}{\partial x} - c_d a h_c U|U|, \tag{20}$$

$$\frac{\partial}{\partial x}\left(Uk - K_a \frac{\partial k}{\partial x}\right) + \frac{\partial}{\partial z}\left(Wk - \mu K\frac{\partial k}{\partial z}\right) = \tau\frac{\partial U}{\partial z} - \epsilon, \tag{21}$$

where K_a is the artificial diffusivity. Comparing with Eqns. (3) and (5) it will be noted that we have dropped several terms arising from the coordinate transformation (i.e. those that vanish as slope $\theta \to 0$) despite our later application of these equations to a hill with slope $\theta \sim H/L \sim 0.4$. Inclusion of those terms is easy, but had no noticeable impact.

(d) *Grid, boundary conditions, discretization and iterative solution*

We used a staggered grid that defines abutting control volumes for U and k (Fig. 2). To avoid questionable specification of the stress on the ground beneath the canopy, we placed the lowest horizontal velocity gridpoint on the ground (direct imposition of the no-slip condition), which allowed us to impose naturally the condition that at the ground the vertical flux of TKE should vanish. Conversely, we set the uppermost U gridpoint in a normal, full, control volume, bounded by the top of the computational domain, so that the upper-boundary condition on U was a specified shear stress. Since a k gridpoint lies on the upper boundary, either (in the case of a field simulation) we specified its value there directly ($k = 1/c_e$), or (in the case of a wind-tunnel) we required $\partial_z k = 0$. In the two-dimensional problem we calculated inflow profiles $U_0(z)$, $k_0(z)$ as equilibrium solutions of the governing equations (more on this below), while at the outflow boundary we set $\partial_x(U, k) = W = 0$.

Our numerical procedure is a variant of the well-tried 'SIMPLE' (semi-implicit method for pressure-linked equations; Patankar 1980). To discretize the governing equations, i.e. to obtain algebraic ('neighbour') equations from the partial differential equations, we firstly integrate *analytically* within a (general) control volume. In that integration, transport terms reduce to influxes/effluxes across control-volume faces (thus our choice of transport form for the equations); the precaution of symmetrical estimation of such

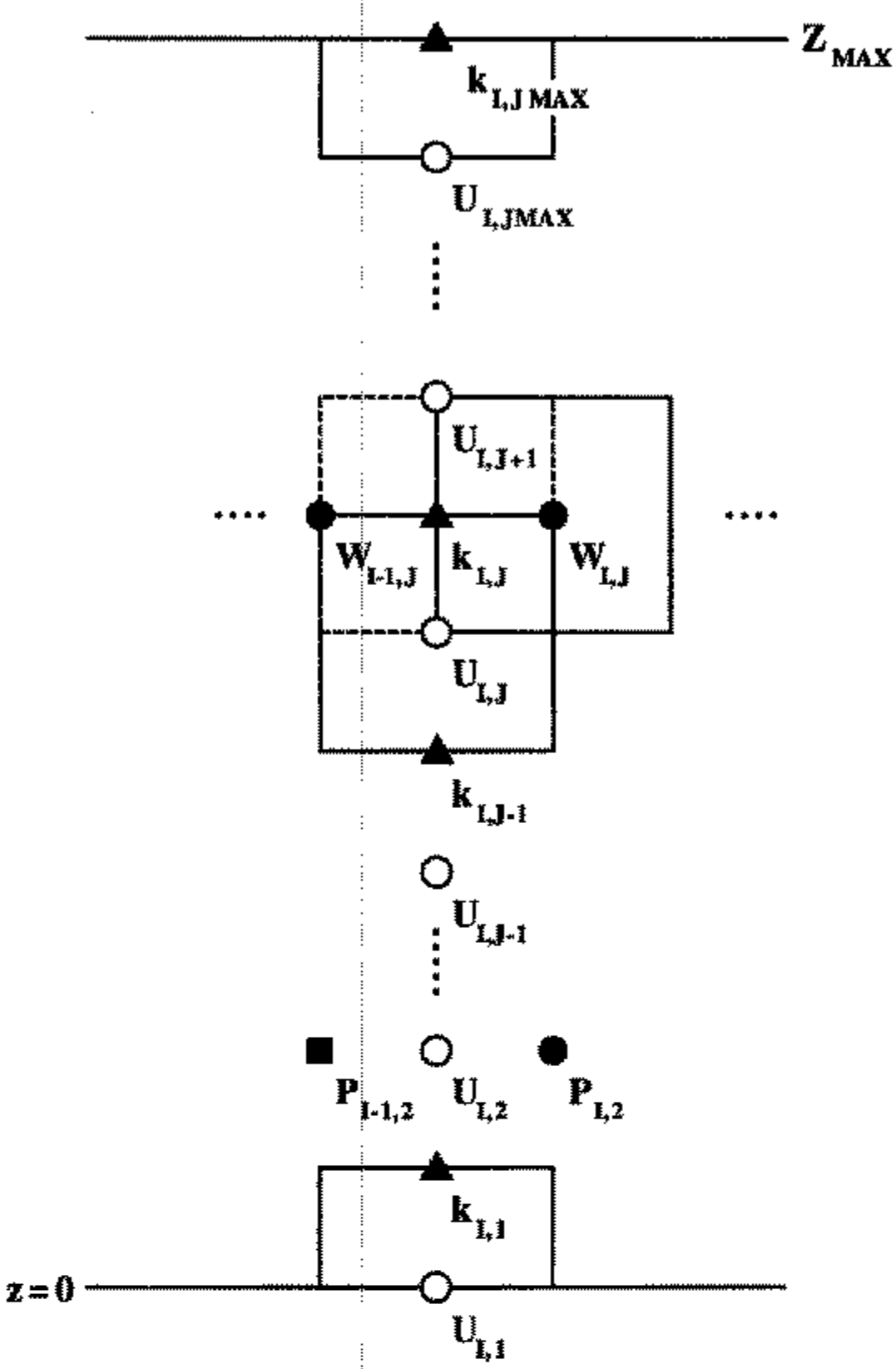

Figure 2. Control volumes and positions of (staggered) gridpoints for mean horizontal and vertical velocity (U, W), pressure (P), and turbulent kinetic energy TKE (k); set up for numerical integration of the U-momentum and TKE equations.

fluxes on either side of the face ensures conservation of all properties, in the absence of source/sink terms.

Let us look at equilibrium solutions of the governing equation, presented later as simulations of the flow in a uniform canopy, and also used as inflow profiles for the disturbed-flow problem. We discard x-derivatives (except of pressure) in Eq. (20), thus for U:

$$\frac{\partial}{\partial z}\left(-K\frac{\partial U}{\partial z}\right) = -\frac{\partial P}{\partial x} - c_d a h_c U|U|. \tag{22}$$

In a 1-dimensional problem, i.e. uniform-canopy flow, the pressure gradient we include above represents any background force present and manifest as a departure of the flow from the idealization of a deep constant-stress layer, such as we consider the undisturbed atmospheric surface layer to be. For example, in a wind-tunnel the effective background force would be a pressure gradient, and/or streamwise advection.

Integrating Eq. (22) with respect to z between z_1 and z_2:

$$\left[-K\frac{\partial U}{\partial z}\right]_{z_1}^{z_2} = \Delta z\left(-\frac{\partial P}{\partial x} - c_d a h_c U|U|\right), \tag{23}$$

where $\Delta z = z_2 - z_1$. The original transport term, now reduced to the difference between the momentum flux across the upper (z_2) plane and the lower, must be estimated by interpolation from values of U (and k) at nearby gridpoints. Let U_j^m be the mth (iterative)

guess at the solution for U at U-grid position z_j. Then the simplest choice is:

$$\left(K\frac{\partial U}{\partial z}\right)_{z=z_2} = K(z_2)\frac{U_{j+1}^m - U_j^m}{\Delta z_n}, \tag{24}$$

where Δz_n is the distance between the jth and $(j+1)$th U-gridpoints, and where $K(z_2)$, the eddy viscosity at the top plane, will involve our coupled estimate of TKE at that position. Writing $U|U| = U_j^m|U_j^{m-1}|$ so as to obtain a linear algebraic equation coupling the neighbouring velocities $(j-1,\ j,\ j+1)$ upon the mth iteration, and collecting terms:

$$A_C^j U_j^m = A_N^j U_{j+1}^m + A_S^j U_{j-1}^m - \Delta z\frac{\partial P}{\partial x}, \tag{25}$$

where the 'North', 'South' and 'Central' neighbour coefficients are:

$$A_N^j = \frac{\lambda(z_2)\sqrt{c_e k^{m-1}(z_2)}}{\Delta z_n}, \tag{26}$$

$$A_S^j = \frac{\lambda(z_1)\sqrt{c_e k^{m-1}(z_1)}}{\Delta z_s}, \tag{27}$$

$$A_C^j = A_N^j + A_S^j + c_d a h_c |U_j^{m-1}|. \tag{28}$$

Of course, special equations prevail on both ends of the z-axis (boundary conditions), while equations of corresponding form link neighbouring values of k. For given matrices k_j^{m-1} and U_j^{m-1} (the 'prior' guess) this constitutes a closed tridiagonal matrix problem for the unknown matrix U_j^m, and may be solved by tridiagonal matrix inversion (for a numerical subroutine see Patankar 1980). Provided some relaxation is provided, i.e.

$$U_j^{m+1} \leftarrow \alpha_R U_j^{m+1} + (1-\alpha_R)U_j^M, \quad \alpha_R < 1, \tag{29}$$

where $\leftarrow$ is to be interpreted as the operation of replacement, this coupled iteration in U, k will converge.

The discretization in two dimensions is analogous, the only complication being the simultaneous presence of convection and diffusion along x (and z in a disturbed problem). Consider a vertical face at $x = x_1$ between the control volume for $U_{i,j}$ on the left and $U_{i+1,j}$ on the right, a boundary across which we will need to specify the total (convective + diffusive) flux, $(UU - K_a\partial_x U)_{x=x1}$. Various possibilities exist for the necessary interpolation; we used Patankar's 'power-law scheme', although since our K_a is small (implying large-grid Peclet number, $P_e = U\Delta x/K_a$), in practice this reduces to an 'upwind' treatment of convection, which eclipses diffusion (along the x-axis).

The neighbour equations involve $U_{i,j}$ and its *four* neighbours. We solved those equations iteratively, setting up matrix inversions that were alternately 'direct' along z and along x. A hillflow situation required approximately 30 s on a Pentium II PC.

3. Experimental data for uniform and disturbed canopies

To judge the utility of the set of simplified-flow equations given above (the 'flow model'), we must specify the closure constants, then compare calculated winds and turbulence with those observed over, preferably, a range of uniform and disturbed flows. We restrict our attention to experiments providing measurements of both the mean flow

and the turbulence (shear stress and TKE), and depend heavily on data from the CSIRO* (Environmental Mechanics) wind-tunnel.

For each experiment we determined a local drag coefficient:

$$c_d a h_c(z) = \frac{1}{U^2(z)} \frac{\partial \tau}{\partial z}, \tag{30}$$

from the measured mean wind and shear stress within the canopy. Because such detailed information on $c_d(z)a(z)$ would usually be unavailable, we also performed simulations using a bulk drag parameter C_d (i.e. a constant value for $c_d a h_c$) defined by:

$$\frac{\tau(h_c)}{u_{*0}^2} = 1 = C_d \int_0^1 \left(\frac{U}{u_{*0}}\right)^2 d\frac{z}{h_c}. \tag{31}$$

From observations of $\sigma_{u,w}$ (and in some cases σ_v) immediately above the canopy, we determined 'equilibrium' ratios $c_u = \sigma_u(h_c)/u_{*0}$, etc., and:

$$c_e = \frac{2}{c_u^2 + c_v^2 + c_w^2}. \tag{32}$$

For future convenience we have tabulated for each experiment the parameters input to our simulations, the experimental profiles U, k, τ, and (derived) C_d, $c_d a h_c(z)$.

(a) *The Furry Hill experiment*

Brunet *et al.* (1994) reported a wind-tunnel study of flow in a model aeroelastic canopy (nylon fishing line) within the CSIRO wind-tunnel-wall boundary layer. In the Furry Hill experiment (Finnigan and Brunet 1995) this canopy was placed upwind and over a Witch of Agnesi ridge. Parameters important for the present work are given in Table 1.

The pressure gradient in the test section of the tunnel upwind of the hill was set to zero by adjusting the height of the tunnel roof, but there was a vertical gradient in Reynolds stress above the canopy (balanced by advection). To permit simulation of the τ, k profiles aloft, for the wind-tunnel experiments we calculated an effective pressure gradient:

$$\frac{1}{\rho u_{*0}^2} \frac{\partial P}{\partial x/h_c} = \frac{\partial}{\partial z/h_c}\left(\frac{\tau_0}{u_{*0}^2}\right) \tag{33}$$

(where ρ is the density and τ_0 is the observed profile of shear stress). This pressure gradient was imposed in the simulations.

(b) *The 'Elora corn' canopy*

Wilson *et al.* (1982) reported profiles of turbulence statistics within (but not above) a mature-corn canopy at Elora, Ontario, using servo-controlled, split-film, heat-transfer anemometers. Here we tested our numerical simulation of canopy flow against the two days of Elora measurements (Tables 2) selected by Wilson (1988), to avoid the complication of changes in canopy height.

For this canopy, leaf-area density $a(z)$ was not height-independent. The profile of $a(z)$ for the time of these measurements is unknown, but in any case, like Wilson (1988) and as for the data from the wind-tunnel experiments, we simply derived from measured $U(z)$ and $\tau(z)$ a profile of the combined parameter $c_d a h_c(z)$, Table 2(C).

* Commonwealth Scientific and Industrial Research Organisation.

TABLE 1. (A) PARAMETERS OF THE FURRY HILL EXPERIMENTS: A MODEL CANOPY ON A RIDGE

Property	Symbol	Value
Hill half-length[1]	L	0.42 m
Hill height	H	0.15 m
Canopy height	h_c	0.047 m
Displacement height	d	0.0333 m
Roughness length	z_0	0.00564 m
Upstream friction velocity	u_{*0}	0.975 m s^{-1}
Canopy drag coefficient[2]	c_d	0.68
Stalk area per volume	a	10 m^{-1}
Bulk drag parameter	$C = c_d a h_c$	0.32
Mean wind at $z = h_c$	$u_0(h_c)/u_{*0}$	3.7 m s^{-1}
Equilibrium variances[3]	$\sigma_{u,v,w}/u_{*0}$	2.2, 2.2, 1.25
TKE at $z = h_c$	$k_0(h_c)/u_{*0}$	5.62
Effective pressure gradient	$(h_c/\rho u_{*0}^2)\partial P/\partial x$	−0.16

[1]The hill profile was truncated at $x/L = \pm 2.20$.

[2]This value for the (bulk) drag coefficient was obtained by Brunet *et al.* (1994) from the measured canopy wind profile and the canopy-top shear stress, assuming zero stress on the ground. They wrote the form drag as $1/2\, c_d a u^2$, and reported $c_d = 1.35$; the value given accords with the practice here of omitting the factor 1/2.

[3]From measurements of $\sigma_{u,w}$ at $z = h_c$, and an approximation that $\sigma_v = \sigma_u$. We ought to have written $\sigma_v^2 = \sigma_u \sigma_w$, as suggested by Legg *et al.* (1984), and as we did for the Tombstone canopy data. However, our inconsistency in the matter of σ_v does not bear on the usefulness of our closure.

TABLE 1. (B) MEAN PROFILES IN AND ABOVE THE FURRY HILL WIND-TUNNEL CANOPY MEASURED AT THE STATION FARTHEST UPSTREAM FROM THE RIDGETOP i.e. $x/L = -5$

z/h_c	U/u_{*0}	τ/u_{*0}^2	k/u_{*0}^2	z/h_c	U/u_{*0}	τ/u_{*0}^2	k/u_{*0}^2
6	11.61	0.17	1.38	1.2	4.56	0.91	5.48
5	10.93	0.32	2.05	1.1	4.24	0.97	5.56
4	10.05	0.44	2.96	1.0	3.7	1.04	5.06
3.5	9.43	0.59	3.62	0.92	3.15	0.9	4.42
3	8.57	0.69	4.18	0.83	2.79	0.76	3.46
2.5	7.61	0.85	4.96	0.75	2.36	0.53	2.64
2.25	7.08	0.85	4.86	0.66	1.87	0.32	1.84
2	6.87	0.78	4.82	0.5	1.47	0.12	1.05
1.75	6.01	0.94	5.26	0.33	1.2	0.06	0.65
1.5	5.51	0.87	5.24	0.16	1.04	0.006	0.38
1.35	5.05	0.94	5.52				

TABLE 1. (C) HEIGHT-DEPENDENT DRAG COEFFICIENT FOR THE FURRY HILL CANOPY (FROM BRUNET *et al.* 1994)

z/h_c	c_d
0.22	0.75
0.4	0.75
0.6	1.1
0.75	0.88
1.1	0

TABLE 2. (A) PARAMETERS OF THE ELORA CORN CANOPY WINDFLOW EXPERIMENTS

Property	Symbol	Value
Canopy height	h_c	2.21 m
Bulk drag parameter	$C = c_d a h_c$	0.79
Mean wind at $z = h_c$	$u_0(h_c)/u_{*0}$	3.04
Equilibrium variances	$\sigma_{u,v,w}/u_{*0}$	2.06, 1.65, 1.13
TKE at $z = h_c$	$k_0(h_c)/u_{*0}^2$	4.12

TABLE 2. (B) MEAN PROFILES IN ELORA CORN 2–4 AUGUST 1977 (WILSON 1988)

z/h_c	U/u_{*0}	τ/u_{*0}^2	k/u_{*0}^2
1	3.04	1	4.12
0.87	2.01	0.87	2.83
0.81	1.58	0.64	2.4
0.75	0.99	0.31	1.46
0.62	0.55	0.12	0.85
0.5	0.4	0.05	0.58
0.44	0.24	0.05	0.37
0.33	0.14	0.02	0.28

Unequal sampling times were used across different levels.

TABLE 2. (C) THE VERTICAL PROFILE OF $c_d(z)a(z)h_c$ DERIVED BY WILSON (1988) FROM MEASURED WIND AND STRESS PROFILES OF THE ELORA CORN CANOPY MEASUREMENTS OF 2–4 AUGUST 1977

z/h_c	$c_d a h_c$	z/h_c	$c_d a h_c$
0.95	0.1	0.5	3
0.9	0.47	0.45	3.6
0.85	1.4	0.4	4.5
0.8	2.3	0.35	5.4
0.75	2.4	0.3	6.6
0.7	2.5	0.25	8.8
0.65	2.6	0.2	16
0.6	2.5	0.15	19
0.55	2.5	0.1	11

The large values deep in the canopy are of dubious validity, deriving from stress *gradient* based on a few small values of shear stress, and setting $c_d a h_c = 4.5$ below $z/h_c = 0.4$ makes negligible change in the simulations.

(c) *The 'Tombstone' canopy*

The 'Tombstone' canopy (Raupach *et al.* 1986) was an array of vertical bars (60 mm high by 10 mm wide), arranged in a regular diamond pattern (spacing 60 mm cross-stream, 44 mm along-stream), on the floor of the CSIRO wind-tunnel. Although an unnatural type of canopy, the experiment provided excellent data on scalar dispersion (trace heat) from line and area sources in the canopy, as well as a test of the importance of horizontal inhomogeneity on the scale of the 'tombstone' spacing. Because this is such an unusual canopy, and because the flow is so comprehensively documented and analysed, these data provide a useful challenge to the breadth of applicability of the closure we have introduced. The parameters are given in Table 3(A).

The flow was in approximate streamwise equilibrium (i.e. along-stream gradients were weak) in the test section. Velocity statistics were measured with a specially developed 3-wire probe (Legg *et al.* 1984). The data used here (Tables 3) are mostly from measurements at (their) $x \approx 1.5$ m. The wind profile is a composite, made up below $z/h_c = 1.5$ of the spatial average $\langle U \rangle$ measured by sonic anemometers at $x = 1.25$ m (their Fig. 3(c); Raupach *et al.* consider this profile their best estimate of wind in the canopy), and made up above $z/h_c = 1.5$ of the hot-wire profile from the central position (D) in the diamond cell at $x = 1.5$ m. TKE and shear stress, likewise, are from $x = 1.5$ m position D. From the

TABLE 3. (A) PARAMETERS OF THE TOMBSTONE CANOPY EXPERIMENTS

Property	Symbol	Value
Canopy height	h_c	0.06 m
Bulk drag parameter	$C_d = c_d a h_c$	0.31
Frontal area per unit volume	a	3.83 m^{-1}
Friction velocity	u_{*0}	1.1 m s^{-1}
Mean wind at $z = h_c$	$u_0(h_c)/u_{*0}$	3.09
Equilibrium variances	$\sigma_{u,v,w}/u_{*0}$	2.0, 1.5, 1.14
TKE at $z = h_c$	$k_0(h_c)/u_{*0}^2$	3.8
Effective pressure gradient	$(h_c/\rho u_{*0}^2)\partial P/\partial x$	−0.23

Friction velocity is derived from measured shear stress above canopy at $x = 1.5$ m. Equilibrium variances assume $\sigma_v^2 = \sigma_u \sigma_w$, as suggested by Legg *et al.* (1984).

TABLE 3. (B) MEAN PROFILES IN AND ABOVE THE TOMBSTONE CANOPY

z/h_c	U/u_{*0}	τ/u_{*0}^2	k/u_{*0}^2	z/h_c	U/u_{*0}	τ/u_{*0}^2	k/u_{*0}^2	$c_d a h_c$
4.45	9.04			1.16	3.82	0.99		
3.78	8.42			1.06		0.97		
3.3	7.83			1	3.09	0.83*		0.19
2.7	6.84			0.96			3.2	0.23
2.3	6.3			0.92				0.27
1.87	5.54			0.9		0.85*		0.29
3.26		0.57		0.85		0.64*	2.74	0.33
2.68		0.78	3.24	0.83	2.27			0.35
2.32		0.75	3.27	0.79				0.38
1.87		0.85		0.72		0.48*	2.2	0.46
1.76			3.25	0.66	1.86	0.39		0.52
1.66	4.91			0.57		0.20, 0.23*	1.66	0.62
1.62			3.71	0.5	1.59			0.27
1.58		0.98		0.42		0.11*	1.19	0.32
1.5	4.54			0.33	1.32			0.14
1.34	4.23	0.95	3.76	0.29			0.98	0.15
1.23		0.86*		0.16	1.18		0.75	0.18

Profiles are measured at streamwise location $x = 1.5$ m, except where noted by an asterisk when they are measured at $x = 2.5$ m.

$c_d a h_c$ is computed from measured stress gradient (composite of τ/u_{*0}^2 profiles at $x = 1.5$, $x = 2.5$ m) and mean wind from sonics and hot wires. Note that our value for the drag coefficient differs from that given by Raupach *et al.* (1986).

vertical gradient in Reynolds stress above the canopy (balanced by advection) we calculated an effective $\partial_x P$.

4. NUMERICAL SOLUTIONS FOR UNIFORM CANOPIES

In this section we determine the three closure constants (c, α, μ) by optimizing a numerical simulation of the upstream (equilibrium) Furry Hill observations, then test them against independent canopy-flow measurements.

According to Launder and Spalding (1972, 1974), the specification $\mu = K_k/K = 1.0$ (equality of eddy viscosity and effective eddy diffusivity for TKE) is optimal for free turbulent flows (plane jets and mixing layers), and also for boundary-layer flows μ 'should be approximately unity'. Notwithstanding those findings, and because we are dealing with a very different flow, we treated μ as free to be varied (more on this below).

The constant α arises due to form-drag. By reasoning similar to Wilson (1988), we expect $\alpha \sim 1$, but its exact value is unknown. Similarly, we have no a priori knowledge of the optimal value of our constant (c) relating the length-scale λ_c to $k^{1/2}(h_c)/(\partial U/\partial z)_{h_c}$. The remaining closure parameter (L_∞) accommodates the (possible) shallowness of the above-canopy constant-stress layer (e.g. in a wind-tunnel). Its numerical value affects our simulated profiles of U, τ, k only far above the canopy in a region of little interest to us. We set $L_\infty/h_c = 1.5$ for numerical simulations of wind-tunnel data; for field experiments, unless one includes a deep layer of the planetary boundary layer (PBL), $L_\infty = \infty$.

In the simulations of this section, the uppermost U gridpoint was placed at $z/h_c = 10$, and vertical resolution was a constant (and unnecessarily generous) $\Delta z/h_c = 0.05$.

(a) *Optimizing closure constants with respect to the Furry Hill upwind observations*

Measurements of U, τ, and k are available to height $z/h_c = 6$, at $x/L = -5$, far upstream from the ridge in the Furry hillflow experiments. Figure 3(a) compares those measured profiles, with simulations using $\alpha = c = 1$, $\mu = 0.2$; all other inputs (d, c_e, c_d, a) are provided unambiguously by the Furry Hill data. The agreement of model and observations is excellent (though the modelled above-canopy gradient in shear stress is only the necessary consequence of our imposed $\partial_x P$). Evidently there is little to be gained by the extra complexity of specifying a height-dependent drag coefficient. The limit-parameter for the in-canopy length-scale is calculated to be $\lambda_c/h_c = 0.36$ and the actual length-scale at canopy top, $\lambda(h_c)/h_c = 0.19$.

In view of the recommendation that $\mu = 1$ (Launder and Spalding 1972, 1974) it is initially surprising that in our flow simulation $\mu = 0.2$ is optimal. The outcome of an alternative parameter choice ($c = 1.5$, $\alpha = 2.5$, $\mu = 1$), visibly inferior in its reproduction of the profile of TKE, is given in Fig. 3(b). However, recall that the diffusivity $K_k = \mu K$ parametrizes the *sum* ($T_p + T_t$) of pressure transport and turbulent transport (of resolved TKE). Now, there are theoretical and experimental grounds for believing these processes partially cancel, i.e. that $|T_p + T_t| < \max\{|T_p|, |T_t|\}$. On theoretical grounds, Lumley (1978) suggested

$$\frac{\overline{p'u'_j}}{\rho} \approx -0.2\,\overline{u'_j u'_k u'_k},$$

and most turbulent wall-layer modelling studies have assumed turbulent transport is dominant. Direct numerical simulation (Rogers and Moser 1994) of a plane mixing layer supported Lumley's suggestion. We believe the mixing layer to be a better analogue of a canopy flow than is a boundary-layer flow, in view of the inflexion-point in the canopy mean wind profile. However observations by McBean and Elliot (1975; p' directly measured) in the unstable atmospheric surface layer, and by Castro and Bradshaw (1976; $\langle p'w' \rangle$ by residual from the TKE equation) on the centre line of a plane mixing layer, gave a much greater role to pressure transport, viz.

$$\frac{\mathrm{d}}{\mathrm{d}z}\overline{p'w'} \approx -\frac{\mathrm{d}}{\mathrm{d}z}\overline{w'(u'^2 + v'^2 + w'^2)},$$

while for the Furry Hill canopy, Brunet *et al.* (1994) inferred (by residual from the TKE budget) that $T_p \approx -0.8T_t$. The crucial point is that, if $|T_p + T_t|/|T_t|$ is systematically different in the canopy from in the simple wall-shear layer, then there is no reason why $\mu = 1$ should obtain. If, as *some* evidence suggests, a larger fraction of T_t than 20% is negated by T_p in canopy (and mixing-layer) flows, then we would require $\mu < 1$, and our specification that $\mu = 0.2$ may be defended.

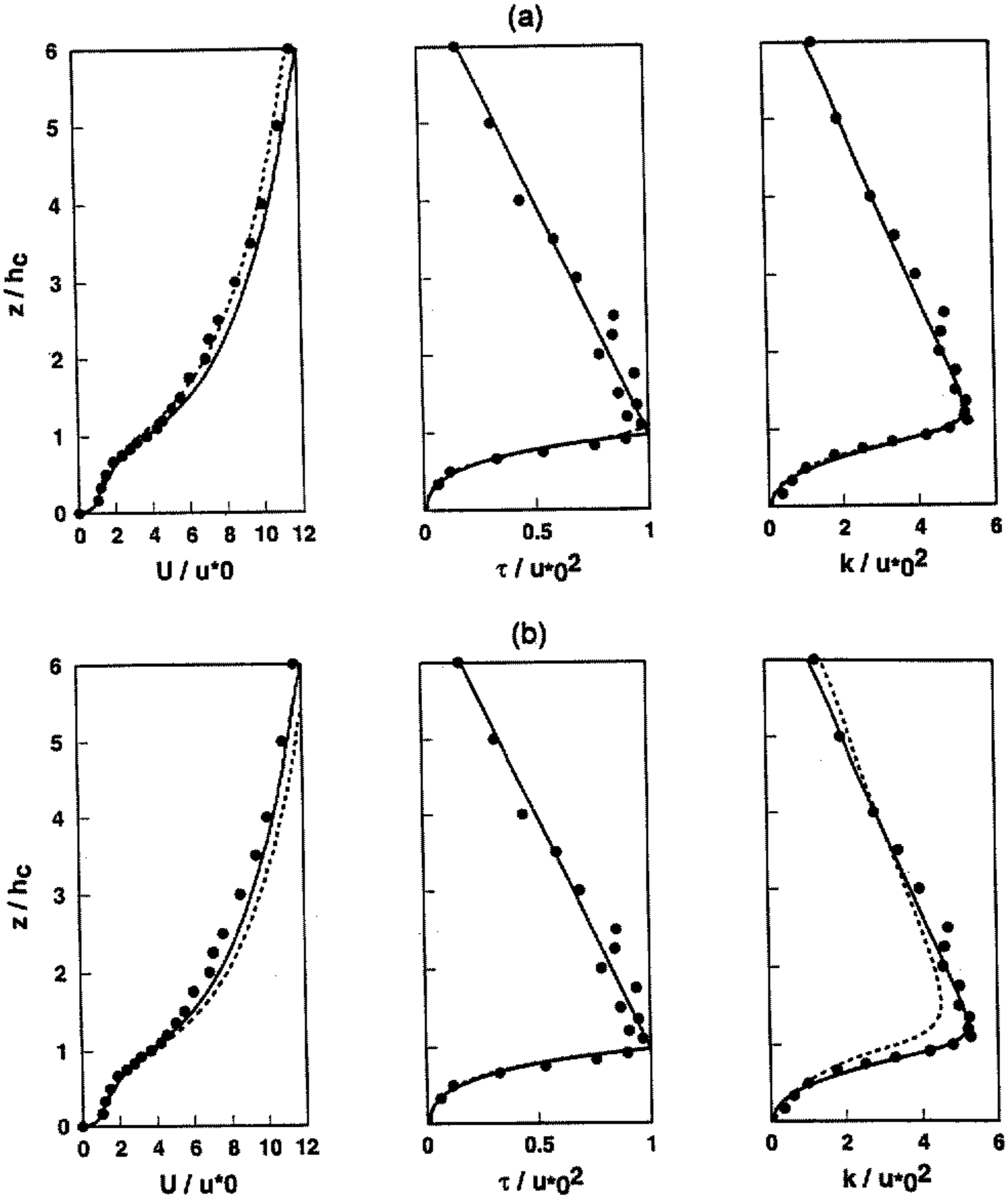

Figure 3. Mean wind speed (U), shear stress (τ), and turbulent kinetic energy (k) observed ($\bullet$) in and above a model aeroelastic plant canopy in a wind-tunnel boundary layer (Furry Hill experiments, data from station $x/L = -5$), compared with the outcome of our numerical simulations. (a) $c = \alpha = 1$, $\mu = 0.2$; and (*solid line*) height-independent bulk drag coefficient $C_d = c_d a h_c = 0.32$ versus (*dashed line*) measured height-variable $c_d a h_c(z)$ from Table 1(C). (b) Height-independent bulk drag coefficient $C_d = c_d a h_c = 0.32$; and (*solid line*) $c = \alpha = 1$, $\mu = 0.2$ versus (*dashed line*) $c = 1.5$, $\alpha = 2.5$, $\mu = 1.0$. See text for further explanation.

Further exploring our reason for setting $\mu = 0.2$, Fig. 4 compares several modelled vertical profiles of the terms in the TKE budget. For each of the parameter choices shown, there is at least *qualitative* agreement with the measured TKE budget of Brunet *et al.* (1994; Fig. 17(b)). In our simulation using $c_d = c_d(z)$, shear production peaks only a little higher than the reported $P(h_c) \approx 4$. Their '$D - P_w$', in which $P_w = -\epsilon_{fd}$, should be compared with the *minimum* of our curves 'D' ($= \epsilon_{cc}$) and 'W' ($= \epsilon_{fd}$), since we set $\epsilon = \max[\epsilon_{cc}, \epsilon_{fd}]$. Then our estimate of the TKE sink is comparable to the profile they observed (peaking at about -6 near the canopy top). And while our TKE balance with $\mu = 0.2$ results in a

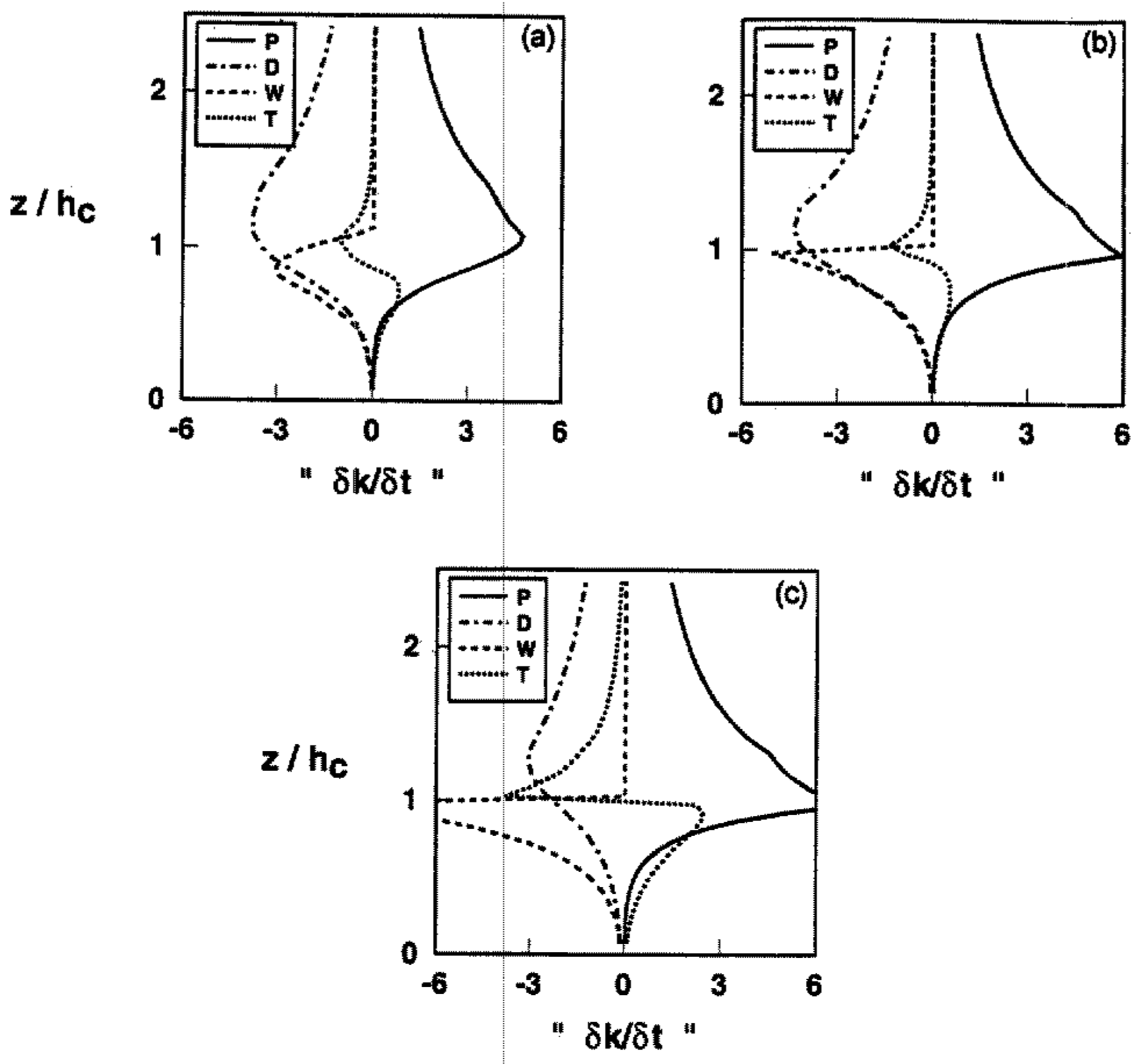

Figure 4. Vertical profiles of terms in the turbulent-kinetic-energy equation, $h_c u_{*0}^{-3} \partial_t k$, according to our simulations of the Furry canopy. P represents shear production, T is turbulent transport, D is ϵ_{cc}, and W is ϵ_{fd}. (a) $c = \alpha = 1$, $\mu = 0.2$, $c_d a h_c(z)$; (b) $c = \alpha = 1$, $\mu = 0.2$, $c_d a h_c = 0.32$; (c) $c = 1.5$, $\alpha = 2.5$, $\mu = 1.0$, $c_d a h_c = 0.32$. See text for further explanation.

smaller transport term (T) than Brunet *et al.* reported, this specification was the only way to match the observed $k(z)$. After considering these TKE budgets, and (more importantly) the simulation of the (directly important and actually observed) variables (U, τ, k), we concluded that within the compass of the present closure scheme, the means to obtain a good simulation of $k(z)$ for the Furry Hill canopy is a reduction of μ from the 'recommended' value. Having 'calibrated' the closure scheme against the Furry Hill data, we now test the model against independent canopy-flow measurements.

(*b*) *Simulation of the Elora corn canopy*

Figure 5 compares modelled ($\alpha = c = 1$, $\mu = 0.2$) and measured profiles of U, τ, and k for the Elora corn canopy. No background pressure gradient was imposed in the simulation, as we expect a constant-stress layer above the canopy in this horizontally uniform flow. In the case of a constant drag coefficient, the limiting in-canopy length-scale was calculated to be $\lambda_c / h_c = 0.24$, and the actual canopy-top length-scale $\lambda(h_c / h_c = 0.15$ (versus 0.36, 0.19 for Furry Hill). Profiles of U, τ resulting from imposition of the 'true' profile $c_d a h_c(z)$ are superior to those using the constant, bulk drag coefficient C_d; and of course, since both specifications derive from observations of U, τ, our modelled profiles

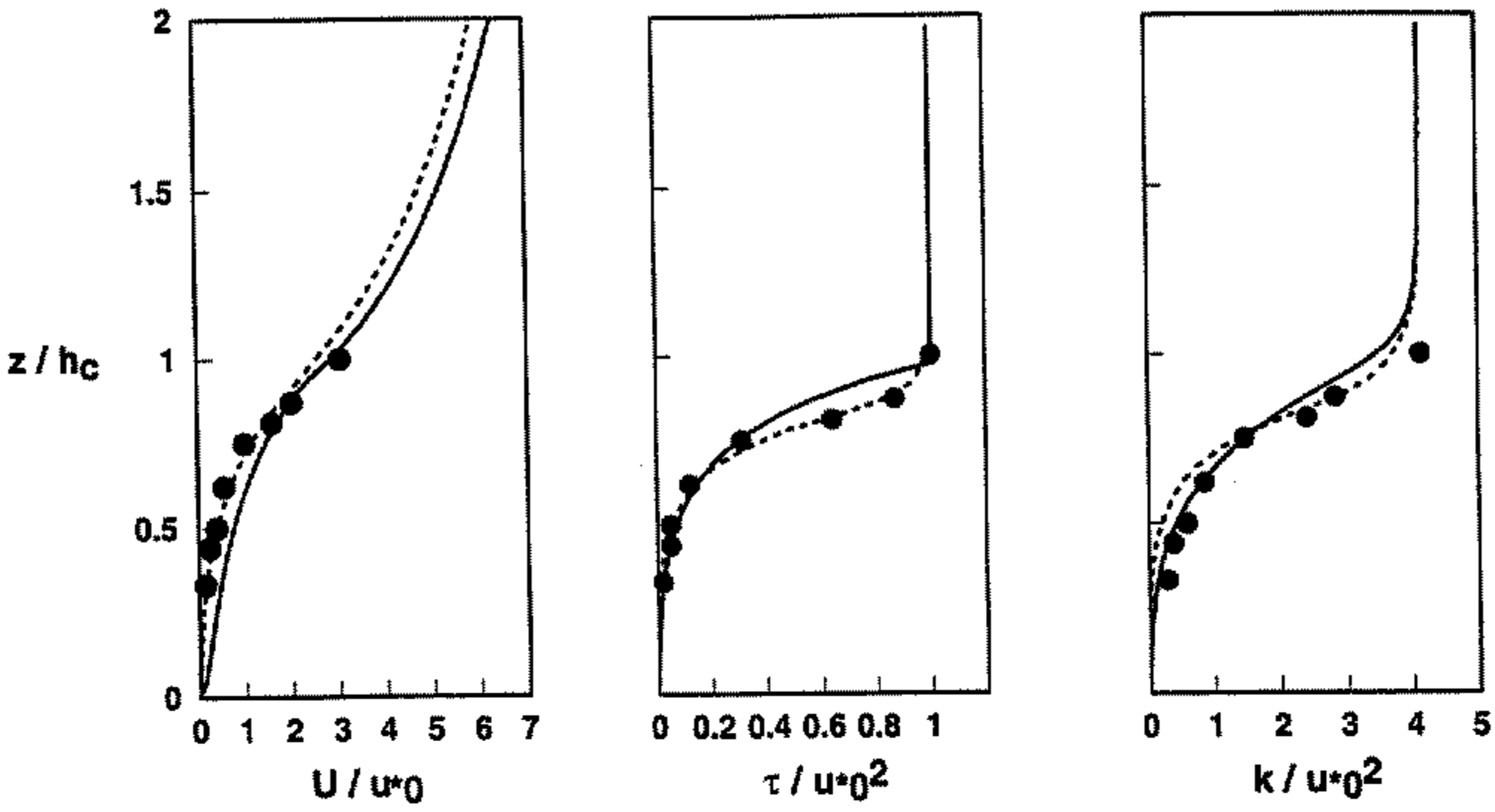

Figure 5. Mean wind speed (U), shear stress (τ), and turbulent kinetic energy (k) observed (•) in a canopy of corn (Elora, Ontario), compared with the outcome of simulations with: $c = \alpha = 1$, $\mu = 0.2$; (*solid line*) height-independent bulk drag coefficient $C_d = c_d a h_c = 0.79$ versus (*dashed line*) measured height-variable $c_d a h_c(z)$ from Table 2(C). See text for further explanation.

of U and τ are not independent. With the height-dependent $c_d a h_c(z)$, if modelled U is 'correct' then so must be modelled τ.

It is pleasing that, without alteration of the closure constants tuned above in line with wind-tunnel measurements, we have achieved a reasonably good simulation of field measurements. Only three program inputs distinguish this simulation from that of the Furry Hill canopy winds: our specification of actual Elora $c_d a h_c$; our specification $c_e = 0.24$ on the basis of the Elora canopy-top data (c_e varies little from flow to flow, and could have been held fixed across our simulations of field and wind-tunnel canopies with very minor impact); and our non-inclusion of a background $\partial_x P$ and a limit to above-canopy length-scale. These last are entirely trivial (and completely appropriate). Thus, to all practical purposes, the *only* distinction of our Elora simulation from that of the Furry Hill wind-tunnel canopy is the inclusion of the correct $c_d a h_c$.

(c) *Simulation of the Tombstone canopy*

A peculiarity of the flow over the Tombstone canopy is that the wind profile aloft is more nearly logarithmic in z than in $z - d$; i.e. the apparent displacement length $d \approx 0$. This conflicts with the report by Raupach *et al.* (1986), but is an unambiguous feature of the mean wind profile near $x = 1.5$ m. Figure 6(a) compares modelled ($\alpha = c = 1$, $\mu = 0.2$; $d = 0$; $L_\infty / h_c = 1.5$) and measured profiles of U, τ, k for the Tombstone canopy, using both a height-dependent and a constant drag coefficient. The model profiles for U, τ are rather good; they are not independent of each other, in view of our specification of the 'true' drag coefficient; and the above-canopy stress gradient is only the necessary consequence of our imposed ∇P. Consistent with the absence of a displacement length in our simulation, our calculated limit to the in-canopy length-scale is markedly higher than for the two previous canopies, $\lambda_c / h_c = 0.48$. Actual canopy-top length-scale is $\lambda(h_c)/h_c = 0.31$, which is nicely consistent with the independent deduction by Coppin *et al.* (1986) from tracer-heat dispersion in this flow, that the Lagrangian time-scale in the canopy is $\tau_L = 0.3 h_c / u_{*0}$.

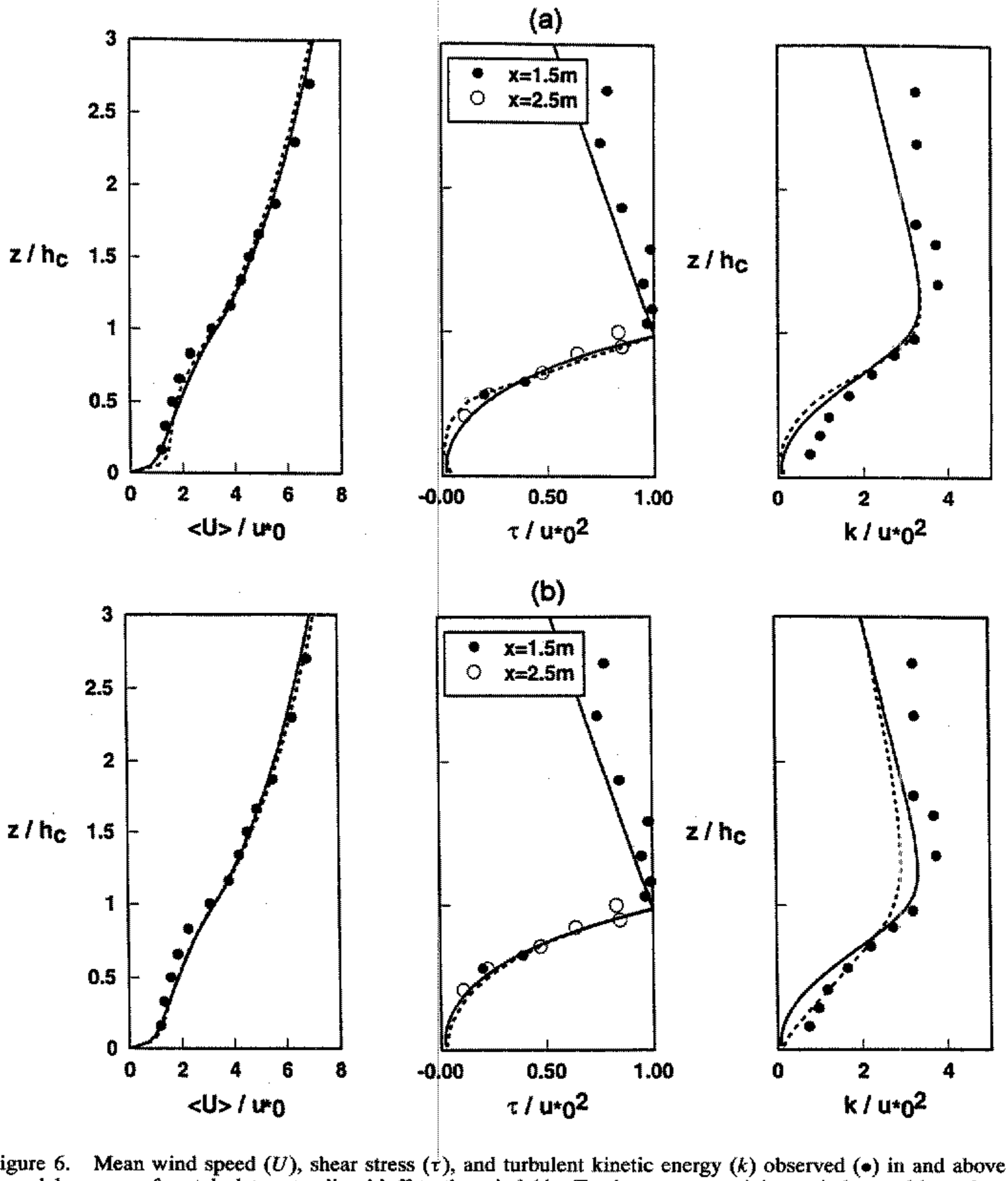

Figure 6. Mean wind speed (U), shear stress (τ), and turbulent kinetic energy (k) observed (•) in and above a model canopy of metal plates standing bluff to the wind (the Tombstone canopy) in a wind-tunnel boundary layer, compared with the outcome of our numerical simulations. (a) $c = \alpha = 1$, $\mu = 0.2$; and (*solid line*) height-independent bulk drag coefficient $C_d = c_d a h_c = 0.31$ versus (*dashed line*) measured height-variable $c_d a h_c(z)$ from Table 3B. (b) Height-independent bulk drag coefficient $C_d = c_d a h_c = 0.31$; and (*solid line*) $c = \alpha = 1$, $\mu = 0.2$ versus (*dashed line*) $c = 1$, $\alpha = 0$, $\mu = 1$ (augmented TKE diffusion, no spectral shortcut). See text for further explanation.

Our underestimation of k deep in the Tombstone canopy is similar to Wilson's (1988, Fig. 8) prediction of $\sigma_u(z)$ for the Tombstone canopy; Wilson used second-order closure and (by oversight!) took z rather than $z - d$ as the length-scale for ϵ_{cc}. In fact, for all three canopies we modelled, our profiles (of U, τ, k) are only *slightly* altered by eliminating the form-drag sink for TKE (setting $\alpha = 0$)—which we tried (firstly) for the Tombstone canopy on the suspicion that the solid, bluff 'tombstones' transferred k, not to irrelevant wake-scales but to larger eddies within the waveband that k itself represents. This surprising result

arises because we wrote $\epsilon = \max[\epsilon_{cc}, \epsilon_{fd}]$. Eliminating the 'spectral shortcut' (Kaimal and Finnigan 1994) due to form-drag, which transfers resolved TKE to invisible small-scale TKE, results in a compensating increase in ϵ_{cc} to an extent which we have not attempted to quantify. Our specification that $\alpha = 1$ is consequently moot.

Figure 6(b) shows that, unsurprisingly, increasing diffusion of k (setting $\mu = 1$) increases k deep in the Tombstone canopy. However because the Tombstone canopy is (aerodynamically) unrepresentative of real canopy flow, and because the choice $\alpha = c = 1$, $\mu = 0.2$ provides a markedly better simulation of the aeroelastic Furry Hill canopy, we prefer the latter specification.

A quibble with the closure we have presented is that, although the chosen form for λ_i gives correct length-scale ($k_v z$) near the ground, it does not result in a *constant* length-scale in the upper-canopy for the canopies considered here (see Fig. 8(b)). That may not be a profound deficiency, but perhaps a different dependence of λ_i upon the guiding factors $k_v z$ and λ_c might be more elegant.

5. Simulations of the Furry hillflow

For the hillflow simulations the (U, k) equations were discretized on a staggered grid spanning $-5 \leqslant x/L \leqslant 5$, $z/h_c \leqslant 15$. Resolution at $(x, z) = (0, h_c)$ was $(\Delta x/L, \Delta z/h_c) = (0.1, 0.05)$; the grid expanded from that point with increasing z and $|x|$. The artificial diffusivity was set at $K_a/u_{*0}h_c) = 10^{-4}$, and the simulations are insensitive to large variations in that parameter.

Recall that our intent is to test the preceding closure scheme, by imposing in the U-momentum Eq. (20) a known pressure gradient, measured in flow over a hill. To that end we can interpolate the actual observations of pressure from the Furry Hill experiments, or use a suitable analytic fit. The theoretical pressure field (P_{JH}) derived by Jackson and Hunt (1975) represents the Furry Hill observations quite well (Fig. 1(a)), provided that an effective hill height $H' < H$ is introduced (because Furry Hill induced separation; note that H' or H enter our simulation in no other way than through our use of P_{JH} as a mere convenience).

Figure 7 shows the observed profiles of U, τ, k along the upslope of Furry Hill, in comparison with a numerical simulation. Closure parameters took our earlier optimized values ($\alpha = c = 1$, $\mu = 0.2$). We used a height-independent drag coefficient; the driving pressure gradient was $\partial_x P_{JH}$ at $x \leqslant 0$, and zero leeward of the hilltop; and to account for the shallowness of the wind-tunnel boundary layer we set $L_\infty/h_c = 1.5$. While there are some deficiencies of our solution (discussed below), overall the agreement of the observations with the calculated response is encouraging. If, rather than P_{JH}, an interpolative fit to the observed ground-level pressure field is used to drive the flow, the simulated windfield is little altered, except most notably in the region $-2 \leqslant x/L \leqslant -1.5$ deep in the canopy, where the observed pressure gradient is more sharply adverse than $\partial_x P_{JH}$ (Fig. 9). Neither does inclusion of the observed height-dependent drag coefficient $c_d(z)$ change the simulation in anything but a very minor way.

The adaptive canopy length-scale $\lambda_c(x)$, used to limit the inner length-scale $\lambda_i(x, z)$, shows an interesting variation over the hillside (Fig. 8(a)), taking near ridgetop a minimum value of about 50% of its equilibrium value (the reduction in $\lambda(h_c)$ is less marked), due to the strongly increased wind shear (at $z = h_c$). Figure 8(b) shows the consequent alteration to the vertical profile of the length-scale $\lambda(x, z)$ at hilltop. The variation in $\lambda_c(x)$ is approximately congruent with the pressure field. That this is so is not surprising. As one of several means we examined for adding a canopy layer to the JH analytical solution, we explored an

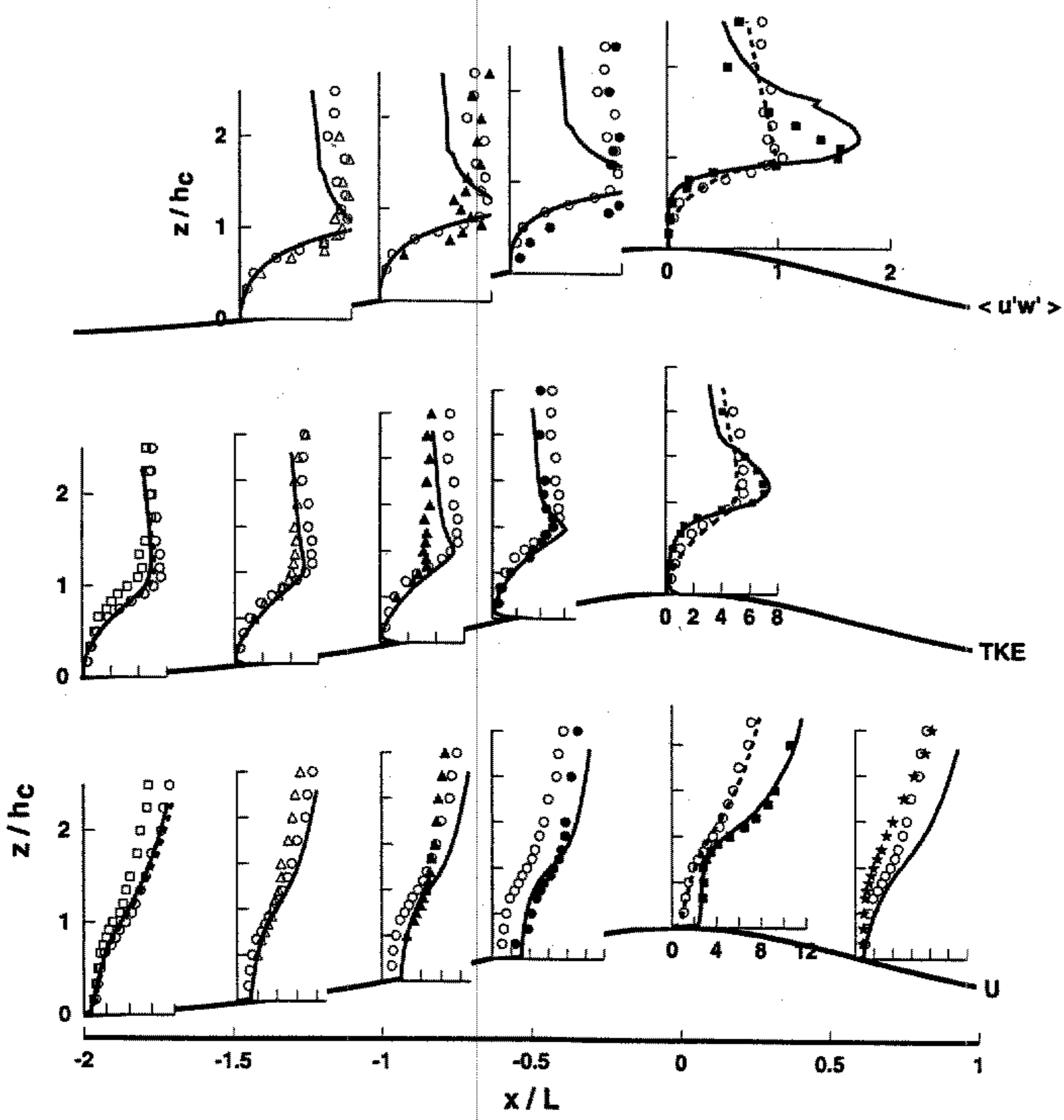

Figure 7. Comparison of observed profiles of mean wind speed (U/u_{*0}), shear stress (τ/u_{*0}^2) and turbulent kinetic energy (k/u_{*0}^2) on Furry Hill with the numerical simulation using $c = \alpha = 1$, $\mu = 0.2$ and height-independent bulk drag coefficient $C_d = c_d a h_c = 0.32$. Solid lines give the local model solution and dashed lines the model equilibrium solution for comparison. At all stations the local observations, represented by the various symbols, are plotted in comparison with the equilibrium-state observations (○), the latter measured upstream from the hill at $x/L = -5$.

analytical treatment of the canopy layer using a momentum-integral method, wherein the canopy-wind profile was presumed *everywhere* to remain of exponential form:

$$U(x, z) = U_{h_c}(x) \exp\left(\beta(x)\frac{z - h_c}{\lambda_c(x)}\right), \tag{34}$$

which is consistent with a height-independent canopy length-scale*. The governing (U, W and continuity) equations provided a single equation, coupling variations in canopy-top

* Unfortunately if a canopy layer, thus treated, is to be matched to the JH treatment aloft, one must set $\lambda_c' = 0$ (there is no perturbation to length-scale in the JH theory).

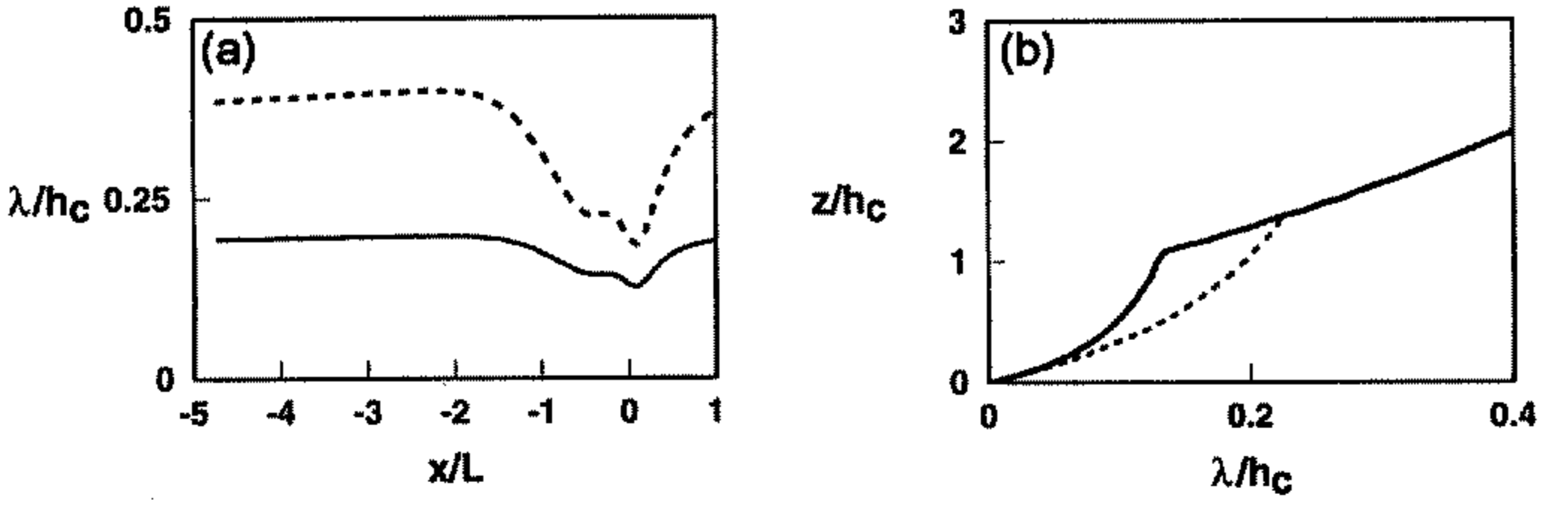

Figure 8. (a) Variation over the Furry hillside of the limit $\lambda_c(x)$ to the in-canopy length-scale (dashed line) and the length-scale at canopy top $\lambda(x, h_c)$ (solid line). (b) Vertical profiles of the length-scale $\lambda(x, z)$ at equilibrium (dashed line) and at hilltop (solid line). See text for further explanation.

mean wind speed $U'_{h_c}(x)$, wind-profile attenuation coefficient $\beta'(x)$, and canopy length-scale $\lambda'_c(x)$ to the driving variation in pressure:

$$n_1\frac{\partial\beta'}{\partial x}+n_2\frac{\partial\lambda'_c}{\partial x}+n_3\frac{\partial U'_{h_c}}{\partial x}=-\frac{\partial P}{\partial x}+n_4\beta'+n_5\lambda'_c+n_6U'_{h_c}, \tag{35}$$

where the real coefficients n_1 to n_6 are dependent only upon the equilibrium properties: $k_v, d/h_c, U_0(h_c)/u_{*0}$. A phase relationship between $P(x)$ and $\lambda_c(x)$ is thus to be expected.

Spatial variation of the canopy length-scale $\lambda_c = \lambda_c(x)$ is not a *crucial* aspect of the success of our simulation. If one specifies $\lambda_c = \text{const}$, the simulation of the perturbed profile of TKE at ridgetop is visibly inferior to that of Fig. 7, but other changes to the profiles are too subtle to be visually distinguishable. In fact, not much is lost by the further simplifications of treating the upwind flow as simply a deep constant-stress layer, and specifying the length-scale as:

$$\begin{aligned}\frac{1}{\lambda(z)}&=\frac{1}{k_v(z-d)} \quad z\geqslant nh_c,\\ &=\frac{1}{k_vz}+\frac{1}{\Lambda} \quad z<nh_c,\end{aligned} \tag{36}$$

with $n\approx 1.5$ and Λ chosen to ensure $\lambda(z)$ is continuous across $z = nh_c$. It is only too easy to culminate with a more complex model than justified by the criterion of agreement with available data.

It can be seen from Fig. 7 that there are interesting variations in the shape of the wind profile over the hill, notably, strong modulation of the wind shear at canopy top, possibly to the extent of *erasing* the inflexion in the wind profile at $x/L\approx -1$, while markedly accentuating the shear (and the inflexion) at hilltop. A qualitative explanation of these effects was given by Brunet *et al.* (1994), and the present work is consistent with their thoughts. In both the canopy layer and in the flow above, the source of disturbance is the *pressure gradient*, set essentially regardless of details of the inner layer on the hill. But there is a mismatch between the response to that pressure gradient of the wind *in* the canopy, and the wind above (see Fig. 9). *Above* the canopy, shear stress (adequately described by our quite simple closure model, or an even simpler one) strongly couples the flow along the vertical, and the force balance is non-local (due to streamwise advection and shear stress); but deep *in* the canopy, where the pressure gradient is unchanged but

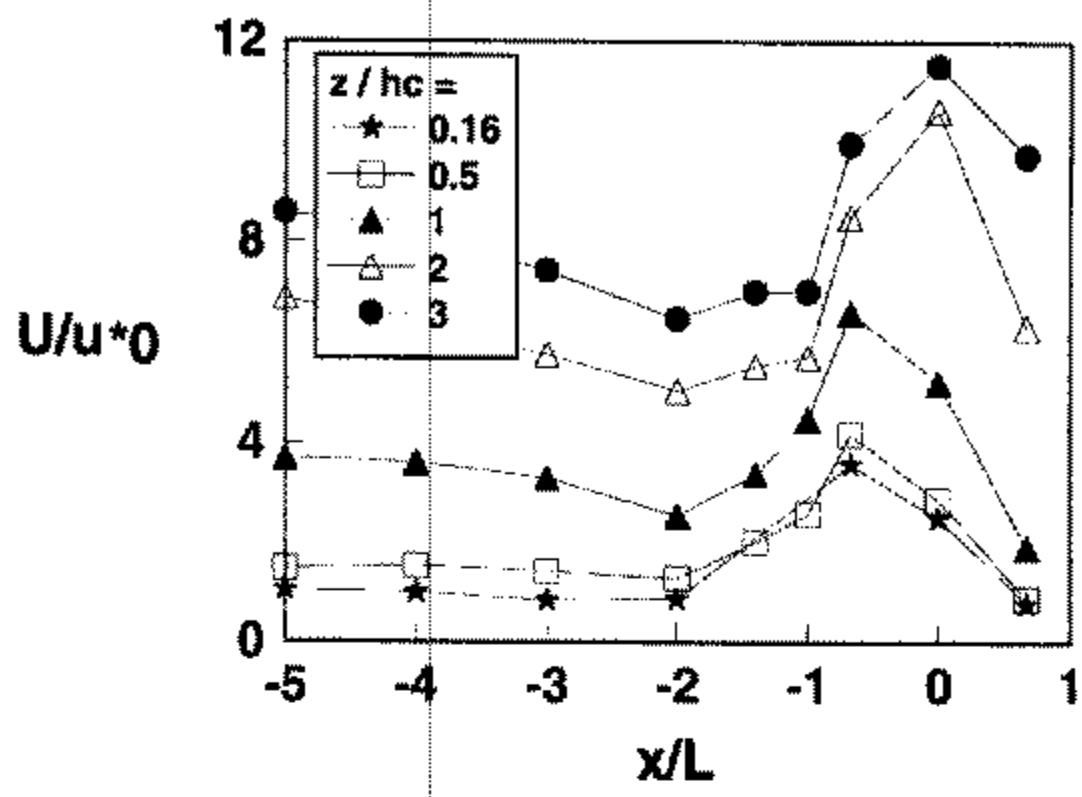

Figure 9. Observed mean velocity field over Furry Hill, showing immediate response of the deep-canopy wind to the pressure gradient $\partial_x P$ (given on Fig. 1(a)) and delayed response by the wind aloft. See text for further explanation.

advection and $\partial\tau/\partial z$ are much smaller terms, the flow is decoupled from aloft, and form-drag strongly moderates the response to the pressure gradient, giving a force-balance in which the 'local' terms (pressure, form-drag) dominate. Thus, strongest winds deep in the canopy appear at the x-location where the pressure gradient is strongest (Fig. 9).

Our model then, seems rather successful: at hilltop its agreement with the observations is striking, certainly capturing the altered shape of the wind profile. Now the model U-profiles are apparently self-congruent in their shape (the inflection point in the U profile near $z = h_c$ is everywhere visible). It is not absolutely clear that the observed wind profile is not also self-congruent; the evidence for erasure of the inflexion point is not compelling. Be that as it may, certainly the strength of the shear at canopy top varies markedly, and is captured by the simulation.

But while the deep-canopy wind is skillfully reproduced everywhere, above the canopy, in the region $x/L \approx -1$, the model changes $U - U_0$ are of opposite sign to those observed, i.e. the model indicates acceleration where deceleration was observed. The JH theory has the same deficiency, and this feature has proven immune to any cure we tried. Please note, however, that we did not attempt to impose on our flow a *height-dependence* of the pressure field such as was actually measured. Thus our failure to predict some details of the response of the wind to flow over the hill may relate to an oversimplification of the pressure field, or (we think improbably) to terms neglected in the equation of motion, rather than (necessarily) to inadequacy of the closure itself.

6. Conclusions

Two key aspects of our numerical solution have permitted much better reproduction of the Furry Hill observations than we obtained in any of the analytical treatments we explored: nonlinearity, and the ability to adopt a height-variable length-scale for the turbulence within the canopy (streamwise adjustment of the length-scale is less important). Because the wind speed deep in the canopy is essentially decoupled from the flow aloft, and governed by the balance of advection, pressure gradient, and form-drag, it is the nonlinearity of the numerical treatment that is the crucial advantage as regards predicting the flow deep in the canopy; the height-variable length-scale $\lambda = k_v z$ of the numerical model near the ground only permits us to resolve the strong shear near the ground (beneath the lowest measurements).

It has been shown elsewhere (Wilson and Flesch 1996) that with a simple alteration to the length-scale $\lambda(x, z)$ in clearings, the closure scheme we have described here also provides a good simulation of the pattern of variation of wind speed and turbulent kinetic energy in periodic forest cut blocks. Thus, perhaps we have established something like the *minimum* level of closure required to calculate disturbances to the wind in a plant canopy. We will recapitulate the basis of these simulations.

We impose the no-slip condition at the ground, and specify either a shear stress or a pressure gradient aloft, as appropriate. Our boundary conditions are otherwise 'neutral', insofar as they do not 'mould' the profiles of U, k, τ. We adopt (and define as c_e^{-1}) the observed equilibrium value at canopy top of k/u_*^2, a quantity that in any case does not greatly vary from canopy to canopy, or from one local equilibrium layer to another. We use measured $c_d a$ to ensure that in the canopy, whatever the wind speed, the 'true' rate of momentum extraction ensues. From those inputs, and given three (at the outset) flexible coefficients, the model produces—with fixed values for those coefficients—quite acceptable profiles of wind, stress, and TKE in equilibrium and disturbed flow. Surely then, the set of reasoned simplifications and choices (length-scale, treatment of vegetation drag, etc.) we applied to the momentum and TKE equations constituting the model, must have captured more than just a grain of truth regarding the simpler types of uniform or disturbed canopy flow. This is surprising, for the closure makes little more than token recognition of the complexity of the flow. Its sole concession to recent thought on (and measurements of) the mechanisms of canopy flow is to invoke the mixing-layer analogy to provide a canopy length-scale. In fact, despite much recent emphasis on the intermittency of canopy flows, and notwithstanding that there are detailed mechanisms at work (e.g. the fluctuating pressure gradients aloft driving deep-canopy wind fluctuations; Shaw and Zhang 1992), on the face of it the striking spatial variations of mean properties can largely be explained by mean advection and 'diffusion' (i.e. parametrized turbulent convection) in the presence of *average* sources (rates of momentum extraction, kinetic energy transformation, etc). This is fortunate, for presumably the vaster framework of large-eddy simulation is a prerequisite if one must do justice to the intermittent processes.

In the context of this simple K-closure, the most uncertain aspect of the implied set of equations is the treatment of TKE sources and sinks in the canopy; these uncertainties are not relieved by using the k-ϵ model, or a higher-order closure; a spectral division of the TKE is called for, as in Wilson (1988). Our practice of writing $\epsilon = \max[\epsilon_{cc}, \epsilon_{fd}]$ is inelegant, and possibly not even advantageous; and we noted that our TKE budget conforms *qualitatively only* with that reported for Furry Hill. Fortunately though, simulations of U, τ are remarkably insensitive to wide variations in treatment of k, possibly because the eddy viscosity is proportional to $k^{1/2}$.

It is appropriate to emphasize again that modified k-ϵ models, although they avoid specification of a turbulence length-scale by carrying an empirical ϵ-equation, suffer from fundamental uncertainty about how best to treat the dissipation mechanisms. For example, the k-equation used by Green (1992) and by Liu *et al.* (1996) included the source term:

$$S_E = c_d a U^3 - 4 c_d a U k,$$

due to plant drag, representing *gain* to k from mean kinetic energy, MKE, and *loss* from k to smaller scales. It is simpler to regard k as *excluding* the TKE residing in fine wake-scales (two-band spectral representation), in which case the MKE conversion term is to be omitted. Ambiguities in similar terms (S_ϵ) of the ϵ-equation are even more serious. Furthermore optimal choices for S_E and S_ϵ are not independent, but are related physically in a manner that is not yet clear.

By no means do we take the success of canopy simulations using an eddy viscosity to imply that higher order closure is worthless. Certainly there could be regions of some flows where turbulent fluxes transfer mean momentum from zones of slow to high mean speed (negative effective eddy viscosity). We will hazard an exploratory suggestion as to where that might occur, from knowing how counter-gradient *scalar* fluxes arise (i.e. by postulating an approximate momentum-scalar analogy). Counter-gradient scalar transport (implying a negative scalar eddy diffusivity) arises in the very near field of distinctly separated sources (Raupach 1987; Wilson 1989) due to the fact that, very near those sources, the net displacement of a marked fluid element relative to its point of release is *not* a sum over many independent random path segments (thus not diffusive), but rather is due to a single path segment along which velocity is highly correlated (memory dominated). Lagrangian treatment of scalar transport completely obviates the difficulties of the Eulerian description, which arise no matter what the order of the (Eulerian) closure.

Whereas scalar concentration of a fluid element is conserved along its trajectory (except for slow changes due to molecular diffusion), even in a nominally inviscid fluid the velocity of a fluid element evolves along its trajectory in response to any pressure field. There is, therefore, no rigorous analogy between momentum transfer and scalar transfer. But despite that reservation let us see where an analogy would take us: where in the PBL do we see widely separated momentum sinks? Momentum sinks only occur near or at the ground. If we looked in great detail at the velocity field between a pair of wires strung above the ground, we might find first-order closure inadequate, at least for suitably contrived spacings. As far as a natural system goes, perhaps the leading edge region of a crop/forest block terminating a long clearing, where there is strong wind penetration, might be a region of counter-gradient transport (near the wake of a strong, vertically distributed momentum sink). This is even more likely if the vertical distribution of the drag is multi-peaked, due to a non-uniform foliage distribution. Ameliorating this putative difficulty, and a compensation not arising in the case of scalar transport, is the fact that in such a region the mean pressure gradient is liable to dominate the behaviour of the flow, so that miscalculation (by a poor closure) of the stresses, which anyway are of secondary importance there, might carry little penalty. Further downwind, with the wind speed throughout much of the canopy being light, the bulk of the drag occurs near canopy top, and there no longer arises a sharply distributed momentum sink. By this line of (strictly unjustifiable) reasoning the eddy viscosity closure might also be unacceptable if we demanded a high fidelity treatment of a very sparse canopy.

In conclusion, we commenced these simulations to guide a parallel search for an analytic description of disturbed canopy flows. A satisfactory analytical solution was not found. But the turbulence closure given here, which is simpler than others claiming comparable effectiveness, captures quite well striking changes to the mean wind in a canopy, caused by flow over hills or through clearings.

Acknowledgements

JDW acknowledges financial support from the Natural Sciences and Engineering Research Council of Canada (NSERC), and from Environment Canada.

References

Ayotte, K. W., Dapeng Xu and Taylor, P. A. 1994 The impact of turbulence closure schemes on predictions of the mixed spectral finite difference model for flow over topography. *Boundary-Layer Meteorol.*, **68,** 1–33

Brunet, Y., Finnigan, J. J. and Raupach, M. R. 1994 A wind tunnel study of air flow in waving wheat: single-point velocity statistics. *Boundary-Layer Meteorol.*, **70,** 95–132

Castro, I. P. and Bradshaw, P. 1976 The turbulence structure of a highly curved mixing layer. *J. Fluid Mech.*, **73,** 265–304

Coppin, P. A., Raupach, M. R. and Legg, B. J. 1986 Experiments on scalar dispersion within a model plant canopy. Part II: An elevated plane source. *Boundary-Layer Meteorol.*, **35,** 167–191

Denmead, O. T. and Bradley, E. F. 1985 Flux-gradient relationships in a forest canopy. In *The forest-atmosphere interaction.* Eds. B. A. Hutchison and B. B. Hicks. D. Reidel, Dordrecht, The Netherlands

Finnigan, J. J. and Brunet, Y. 1995 Turbulent airflow in forests on flat and hilly terrain. Pp. 3–40 in *Wind and trees.* Eds. M. P. Coutts and J. Grace. Cambridge University Press, UK

Gardiner, B. A. 1994 Wind and wind forces in a plantation spruce forest. *Boundary-Layer Meteorol.*, **67,** 161–186

Green, S. R. 1992 Modelling turbulent airflow in a stand of widely-spaced trees. *PHOENICS J. Comp. Fluid Dyn. and Applic.*, **5,** 294–312

Holland, J. Z. 1989 On pressure-driven wind in deep forests. *J. Appl. Meteorol.*, **28,** 1349–1355

Jackson, P. S. and Hunt, J. C. R. 1975 Turbulent wind flow over a low hill. *Q. J. R. Meteorol. Soc.*, **101,** 929–955

Kaimal, J. C. and Finnigan, J. J. 1994 *Atmospheric boundary layer flows.* Oxford University Press, UK

Kobayashi, M. H., Pereira, J. C. F. and Siqueira, M. B. B. 1994 Numerical study of the turbulent flow over and in a model forest on a 2D hill. *J. Wind Eng. Indust. Aero.*, **53,** 357–374

Launder, B. E. and Spalding, D. B. 1972 *Mathematical models of turbulence.* Academic Press, London, UK

1974 The numerical computation of turbulent flows. *Comput. Methods Appl. Mech. Eng.*, **3,** 269–289

Launder, B. E., Reece, G. J. and Rodi, W. 1975 Progress in the development of a Reynolds-stress turbulence closure. *J. Fluid Mech.*, **68,** 537–566

Legg, B. J., Coppin, P. C. and Raupach, M. R. 1984 A three-hot-wire anemometer for measuring two velocity components in high intensity turbulent boundary-layers. *J. Phys. E.*, **17,** 970–976

Liu, J., Chen, J. M., Black, T. A. and Novak, M. D. 1996 E-ϵ modelling of turbulent air flow downwind of a model forest edge. *Boundary-Layer Meteorol.*, **77,** 21–44

Lumley, J. L. 1978 Computational modelling of turbulent flows. *Adv. Appl. Mech.*, **18,** 123–176.

McBean, G. A. and Elliot, J. A. 1975 The vertical transports of kinetic energy by turbulence and pressure in the boundary layer. *J. Atmos. Sci.*, **32,** 753–766

Meyers, T. and Paw U, K. T. 1986 Testing of a higher order closure model for modelling airflow within and above plant canopies. *Boundary-Layer Meteorol.*, **37,** 297–311

Monin, A. S. and Yaglom, A. M. 1977 *Statistical fluid mechanics.* The M.I.T. Press, USA

Patankar, S. V. 1980 *Numerical heat transfer and fluid flow.* Hemisphere Publ. Co., London, UK

Raupach, M. R. 1987 A Lagrangian analysis of scalar transfer in vegetation canopies. *Q. J. R. Meteorol. Soc.*, **113,** 107–120

Raupach, M. R., Coppin, P. A. and Legg, B. J. 1986 Experiments on scalar dispersion within a model plant canopy. Part I: The turbulence structure. *Boundary-Layer Meteorol.*, **35,** 21–52. See also erratum, *Boundary-Layer Meteorol.*, **39,** 423–424

Raupach, M. R., Finnigan, J. J. and Brunet, Y. 1996 Coherent eddies and turbulence in vegetation canopies: the mixing-layer analogy. *Boundary-Layer Meteorol.*, **78,** 351–382

Rogers, M. M. and Moser, R. D. 1994 Direct simulation of a self-similar turbulent mixing layer. *Phys. Fluids*, **6,** 903–922

Shaw, R. H. and Seginer, I. 1985 'The dissipation of turbulence in plant canopies.' Pp. 200–203 in Proceedings of the 7th Symposium on Turbulence and Diffusion, Am. Meteorol. Soc., Boulder, USA

Shaw, R. H. and Zhang, X. J. 1992 Evidence of pressure-forced turbulent flow in a forest. *Boundary-Layer Meteorol.*, **58,** 273–288

Svensson, U. and Haggkvist, K. 1990 A two-equation turbulence model for canopy flows. *J. Wind Eng. Indust. Aero.*, **35,** 201–211

Taylor, P. A. 1977 Some numerical studies of surface boundary-layer flow above gentle topography. *Boundary-Layer Meteorol.*, **11,** 439–465

Taylor, P. A., Mason, P. J. and Bradley, E. F. 1987 Boundary-layer flow over hills. *Boundary-Layer Meteorol.*, **39,** 107–132

Wilson, J. D. 1988 A second-order closure model for flow through vegetation. *Boundary-Layer Meteorol.*, **42,** 371–392

1989 Turbulent transport within the plant canopy. In *Estimation of areal evapotranspiration*. Intl. Assoc. Hydrol. Sci. Publication. No 177, 43–80

Wilson, J. D. and Flesch, T. K. 1996 'Diagnosing wind variation in periodic forest clearcuts, in relation to tree sway.' Pp. 387–390 in preprint volume of 22nd Conference on Agricultural and Forest Meteorology, Am. Meteorol. Soc., Atlanta, USA

Wilson, N. R. and Shaw, R. H. 1977 A higher order closure model for canopy flow. *J. Appl. Meteorol.*, **16,** 1197–1205

Wilson, J. D., Ward, D. P., Thurtell, G. W. and Kidd, G. E. 1982 Statistics of atmospheric turbulence within and above a corn canopy. *Boundary-Layer Meteorol.*, **24,** 495–519

Wilson, J. D., Finnigan, J. J. and Raupach, M. R. 1995 'Exploratory models of windflow through a plant canopy on a ridge.' Pp. 539–542 in preprint volume of 11th Symposium on Boundary Layers and Turbulence, Am. Meteorol. Soc., Charlotte, USA

Ying, R., Canuto, V. M. and Ypma, R. M. 1994 Numerical simulation of flow data over two-dimensional hills. *Boundary-Layer Meteorol.*, **70,** 401–427